Supporting Information

Electrocatalyst decomposition pathways: torsional strain in a second sphere proton relay shuts off CO2RR in a Re(2,2'-bipyridyl)$(CO)_3$X type electrocatalyst

Zachary Dubrawski, Chia Yun Chang, Cody Carr, Benjamin S Gelfand and Warren E. Piers*
Department of Chemistry. University of Calgary, 2500 University Drive NW, Calgary, AB, T2N 1N4, Canada
*Corresponding authors:
wpiers@ucalgary.ca

Contents

General Considerations

Materials and Reagents

Air and moisture-sensitive reactions were carried out under an argon atmosphere using standard schlenk line techniques. Tetrahydrofuran was dried over activated alumina using a solvent purification system and stored in 500 mL thick-walled glass vessels over sodium/benzophenone ketal. Acetonitrile was dried over CaH_2. All solvents were degassed and vacuum distilled prior to use. 2-amino-3-bromobenzaldehyde was purchased from Combi-Blocks and used without further purification. $Re(CO)_5Cl$ was purchased from Sigma-Aldrich, stored under inert atmosphere in an Ar filled glovebox and used without further purification. Decamethylcobaltocene and potassium tert-butoxide was purchased from Sigma-Aldrich and sublimed prior to use. KC_8 was prepared according to literature procedures.[1] **1** was purchased from Combi-Blocks and used as received. **i** and **ii** were prepared according to literature reports with some modifications detailed below. [2,3] $Re(bpy)(CO)_3Cl$ synthesized according to literature procedure.[4]

Electrochemistry

All electrochemical measurements were performed on a CHI 660D or 660E potentiostat at room temperature (20 ± 2 °C) in a three-electrode configuration. A carbon-based working, Pt mesh counter and Ag/AgCl wire reference electrode were used in dry dimethylformamide (DMF) containing 0.1 M $TBAPF_6$ (Sigma, electrochemical grade, ≥99.0%) as supporting electrolyte and 1.0 mM analyte (for experiments with Re complex in solution). The Ag/AgCl wire was immersed into a glass tube filled with electrolyte solution and separated *via* a CoralPor frit from the analyte-containing solution. Ferrocene (Fc) was added as an internal standard at the end of each measurement, and potentials were referenced against the Fc^+/Fc redox couple (0 V). Cyclic voltammograms were recorded in a glovebox under Ar atmosphere (unless otherwise noted), and, in case of CO_2 atmosphere, solutions were purged with CO_2 (Air liquide, Research grade) for 10 min. Redox potentials are reported as peak potential of the cathodic wave (E_{pc}) except when otherwise specified. Controlled potential electrolysis (CPE) was performed in a two-compartment cell (Re complex in solution) with an ultra-fine frit separating the two compartments. The Pt mesh counter electrode was placed into the anodic compartment filled with electrolyte solution (8 mL DMF/0.1 M $TBAPF_6$). A glassy carbon plate working (2 cm depth immersed into solution) and the Ag/AgCl reference electrode were placed into the cathodic compartment containing the analyte solution (8 mL, 0.5 mM catalyst, DMF/0.1 M $TBAPF_6$). After sealing the cells with rubber septa, solutions were purged with CO_2 for 15 min. The remaining headspace was regularly sampled (50 µL) using a gastight Hamilton syringe and analysed via gas chromatography. After CPE the electrodes were tested for electrochemically active precipitates with the rinse test.

Electrode preparation

Glassy carbon disks (3 mm, PEEK-encased, BaSi) and glassy carbon plates (Alfa Aesar, type 1, thickness = 2 mm) were polished before each experiments using 0.3 µm alumina paste on a microfiber cloth. For solution experiments, the glassy carbon disks were cleaned between each cyclic voltammetry run. CPE GC plates were attached to a steel rod with electrically conductive Cu tape, wrapped in Teflon tape and then Parafilm. Acceptable conductivity through the prepared electrode was confirmed before starting a CPE experiment

Gas chromatography

The gas chromatograph (GC, Agilent 7890B Series) was equipped with a PoraPlot Q and PLOT molecular sieve (5 Å) column (oven temperature 60-120 °C) and a VICI pulse discharge Helium ionization detector

(PDHID). Helium (5.0) was used as carrier gas at a flow rate of approx. 5 mL min^{-1}. The GC was calibrated in regular intervals with known CO_2-balanced gas mixtures containing H_2 and CO. All experiments were performed at least in triplicate (unless otherwise noted). See below for statistical analysis.

Spectroelectrochemistry

Experiments were conducted using a LabOmak SEC OTTLE cell fitted with CaF_2 windows, Pt working and counter electrode, and Ag wire pseduoreference electrode which was reference to an external sample of Fc^+/Fc. The optical pathlength is 0.2mm which was filled with 0.3M $TBAPF_6$ DMF solutions as background. The background and analyte solutions were prepared in an argon filled glovebox. The cell was also assembled in the glovebox and CVs taken of background DMF samples show no O_2 reduction present. CO_2 sparged solutions were prepared by bubbling the DMF solutions with anhydrous CO_2 and quickly added to the cell. Significant bubble formation in the window is observed with CO_2 sparged solutions.

IR spectroscopy
Infrared spectra were recorded on an Agilent Cary 630 FT-IR spectrometer with a transmission setup (SEC and solution samples). A background of solvent was recorded prior to measuring the Re complex. Spectra were averaged over 145 scans with a resolution of 2 cm^{-1}. Spectra were averaged over 64 scans with a resolution of 4 cm^{-1} and processed using the OMNIC 9.2 software package provided with the instrument. A background scan was recorded before each sample scan.

NMR spectroscopy
^1H and ^{13}C NMR spectra were recorded on a Bruker AV-III 500 MHz or 600 MHz NMR spectrometer at room temperature (r.t.). The measurements were carried out in commercially available deuterated solvents. ^1H and ^{13}C NMR spectrometry chemical shifts were referenced to residual proteo-solvent resonances and naturally abundant ^{13}C NMR resonances for all deuterated solvents.

X-Ray crystallography
Data were collected with Cu Kα radiation on a Bruker Smart diffractometer equipped with an Apex II CCD detector, fixed-CHI goniometer, and sealed-tube (Cu) source. The crystal was kept at 173.0 K during data collection. Using Olex2,[2] the structure was solved with the ShelXT[3] structure solution program using Intrinsic Phasing and refined with the XL[4] refinement package using least squares minimization. Structures can be accessed from the accession numbers 2175393-2175398

Other physical measurements
Elemental analyses and high-resolution mass spectra were obtained at the Instrumentation Facility in the Department of Chemistry, University of Calgary. Mass spectra were recorded in methanol (organic compounds) or acetonitrile (Re complex).

pK_a Determination

A 20 mL scintillation vial was charged with **1** in a quantity of fresh d_6-DMSO. The solution was partitioned into NMR tubes and exposed to bases with known conjugate acid pK_a. The bases and reported pK_a are reported below. Reported p pK_a's were found from the convenient tables made by Dr. Hans Reich which includes references found here. The NMR spectra of the resultant solutions is Fig S19

Table S1: The deprotonation of **1** with various weak bases

Base	Reported pK_a in DMSO of conjugate acid	Rxn with **1** to generate deprotonated complex	Reference for pKa
NaOAc	12.3	Yes	[5]
NEt_3	9.0	Yes	[6,7]
Proton Sponge	7.5	Incomplete Reaction (see notes below)	[8]
Pyridine	3.4	No	[9]

The reaction of **1** and proton sponge does not go to completion, rather two products and starting material are observed in solution. By NMR, one product is the deprotonated species and we presume the other to be the Proton Sponge adduct. This makes quantitation difficult as the species are not only in equilibrium with protonated/deprotonated products, but also adducts/dimers. Therefore, to hedge our bets, we report the pK_a of **1** to be a range between trimethylamine (pK_a = 9) and Proton Sponge (7.5) to avoid inaccuracies in our BDFE measurements. Despite this admittedly higher-than-reality pK_a, the BDFE is still low enough to allow for spontaneous H2 evolution observed in the synthesis of **2.**

The electrochemistry of **1** is performed in DMF and while not much variance in pKa should be expected between DMSO and DMF, the synthesis of **2** is performed in C_6H_6 and as such, there could be a wide discrepancy in pK_a values.[10] Unfortunately, the pK_a of simple acids are not well studied in non-polar solvents. There are some reports of aryl N-H pK_a determination in n-heptane, which may be used as a model for C_6H_6 in the absence of better alternatives. In heptane, the N-H pK_a were found to be far more acidic than in DMSO, with an approximate change of -4 pK_a units.[11,12] Accordingly, we would expect the BDFE of **1** to fall with the increase in acidity, perhaps lowering the estimated BDFE even further. We acknowledge that the pK_a estimated above is for **1** and not the singly reduced species however, we anticipate that while the pK_a should rise due to unfavourable charge accumulation, it should still be within a range to accommodate loss of the H· radical.

Equations

Experiments performed in triplicate (unless otherwise noted) with average values and standard deviations reported.

$$\boldsymbol{x_u} = \sum_i \frac{\boldsymbol{x_i}}{\boldsymbol{n}} \qquad \boldsymbol{\sigma} = \sqrt{\sum_i \frac{(\boldsymbol{x_i}-\boldsymbol{x_u})^2}{(\boldsymbol{n}-\boldsymbol{1})}}$$

Where x_u = unweighted mean value, x_i = obervations, n = number of observations and σ = standard deviation

Faradaic Efficiency

$$FE(\%) = \frac{n(CO)_{meas}}{n(CO)_{calc}} \cdot 100\% = \frac{n(CO)_{meas}}{\frac{Q}{zF}} \cdot 100\%$$

Where Q = charge passed over course of CPE experiment, z = # electrons required for reduction to CO = 2, and F = Faradaic Constant

Determination of k_{obs}using i_c/i_p analysis[13]

$$\frac{i_{cat}}{i_p} = 2.2406\sqrt{\frac{RT}{nFv}}n'k_{obs}$$

Where i_{cat} = peak current of redox wave under catalytic conditions, i_p = peak current of redox wave, R = universal gas constant, T = temperature, n = # electrons transferred, F = Faradaic constant, v = scan rate, n' = # of catalyst molecules required per turnover (presumed to = 1), k_{obs} = observed rate constant as defined in reference S**.

Bordwell Equation for Bond Dissociation Free Energy[14]

$$BDFE_{solv}(X-H) = 1.37pK_a + 23.06E^o + C_{G,sol}$$

Where pKa is for the X-H bond of interest, E^o is the standard potential of the analyte (the average of anodic and cathodic peaks in CV for the redox event, defined as $E_{1/2}$, is typically used as a good measure of E^o), and $C_{G,\,solv}$ is a solvent dependant constant ($C_{G,DMF}$ = 69.7 kcal/mol)

Synthesis of Compounds

Synthesis of 2-pyridyl-8-bromoquinoline, i

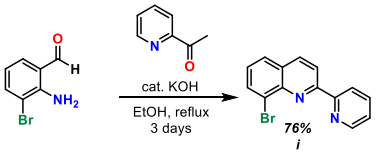

Synthesis has been adapted from Thummel et al. 5.001 g (1 eq., 0.025 mol) 2-amino-3-bromobenzaldehyde, 3.789 g acetylpyridine (1.3 eq, 0.031 mol) and 0.778 g potassium hydroxide (0.5 eq., 0.014 mol) was combined in 200 mL 90% ethanol. The suspension was heated to reflux for 3 days. The reddish-brown solution was cooled to room temperature and the solvent removed under reduced pressure. The oily, extremely sticky solid material was transferred to a sublimation apparatus and **i** readily sublimed at 100°C at 30 mTorr pressure. Analytically pure **i** was obtained from the cold finger as a white, free-flowing powder. NMR spectra matched previous reports Final yield = 5.41 g, 0.018 mol, 76%

^{1}H NMR (500 MHz, $CDCl_3$) δ 8.86 (d, *J* = 8.0, 1H), 8.73 (d, *J* = 4.9 Hz, 1H), 8.66 (d, *J* = 8.6 Hz, 1H), 8.28 (d, *J* = 8.6 Hz, 1H), 8.07 (dd, *J* = 7.4, 1.3 Hz, 1H), 7.91 (td, *J* = 7.7, 1.8 Hz, 1H), 7.82 (dd, *J* = 8.1, 1.3 Hz, 1H), 7.43 – 7.35 (m, 2H).

Synthesis of AbP, ii

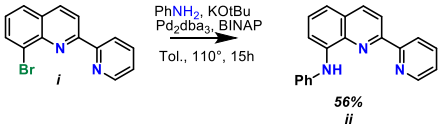

0.500 g **i** (1 eq., 0.0017 mol), 0.056 g Pd_2dba_3 (3%, 0.03 eq, 6. 1e-5 mol), 0.076 g rac-BINAP (7%, 0.07 eq, 12e-4 mol), 0.235 KOtBu (1.2 eq, 0.0021mol), 0.195 g aniline (1.2 eq. 0.021 mol) were combined in a thick-walled glass bomb along with 15 mL dry toluene. The solution was heated to 110°C overnight. After cooling to room temp, the mixture was diluted with DCM and flashed through a silica plug with more DCM to remove the bulk of palladium. The solvent was removed to give a brown oil, which was purified by flash column chromatography (3:2 hexane: Et_2O) to give a bright yellow solid. This solid was treated with the silica adsorbed Pd-scavenging agent, SiliaMet-Thiol, according to manufacturer's instructions (room temperature mix in DCM overnight). Finally, **3** was recrystallized from hot MeOH. NMR Spectra match previous reports. Final yield = 0.292 g, 0.00098 mol, 56%

^{1}H NMR (500 MHz, $CDCl_3$) δ 8.75 (d, *J* = 4.6 Hz, 1H), 8.64 (d *J* = 8.0 Hz, 1H), 8.60 (d, *J* = 8.6 Hz, 1H), 8.37 (bs, 1H), 8.26 (d, *J* = 8.6 Hz, 1H), 7.89 (td, *J* = 7.7, 1.8 Hz, 1H), 7.53 – 7.32 (m, 7H), 7.09 (tt, *J* = 7.2, 1.3 Hz, 1H).

UV-Vis$_{DMF}$: λ_{max} = 410 nm (520 $M^{-1}cm^{-1}$)

Synthesis of Re(AbP)(CO)$_3$Cl, 1

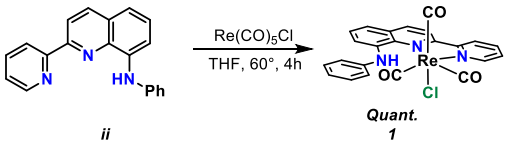

In an argon filled glovebox, 150 mg **ii** (5.0e-4 mol, 1.0 eq) and 174 mg Re(CO)$_5$Cl (4.8e-4 mol, 0.95 eq) were combined with 30 mL anhydrous THF in a 100 mL Schlenk flask with a teflon Kontes tap. The solution was heated to reflux for 4 hours before cooling to room temperature and opening to atmosphere. The solvent was removed under reduced pressure and the purple solid was triturated with hexane to remove excess **ii**. The compound can be recrystallized from Et2O:pentane. Final yield = 0.289 g, mol, 100% based on Re starting material used.

^{1}H NMR: 1H NMR (500 MHz, CDCl3) δ 9.18 (d, J = 5.5 Hz, 1H), 8.75 (s, 1H), 8.52 (d, J = 8.6 Hz, 1H), 8.18 – 8.12 (m, 2H), 8.07 (d, J = 8.6 Hz, 1H), 8.00 (dd, J = 8.1, 1.3 Hz, 1H), 7.65 (ddd, J = 7.2, 5.4, 1.9 Hz, 1H), 7.57 (t, J = 8.0 Hz, 1H), 7.55 – 7.49 (m, 2H), 7.43 (t, J = 7.9 Hz, 2H), 7.37 (dd, J = 7.9, 1.3 Hz, 1H), 7.13 (t, J = 8.1 Hz, 1H).

^{13}C NMR (126 MHz, CDCl$_3$) δ 195.13, 193.96, 188.05, 156.58, 156.27, 152.75, 140.92, 140.70, 140.21, 138.90, 138.12, 130.32, 129.70, 128.65, 126.25, 123.71, 122.99, 121.99, 117.63, 115.68, 110.97.

IR (KBr Pellet): v(CO) = 2022, 1916, 1886. v(N-H) = 3270

IR soln: v(CO) = 2022, 1918, 1893. v(N-H) in DCM = 3275

UV-Vis$_{DMSO}$: λ_{max} = 514 nm (2710 M^{-1}cm^{-1})

ESI-Mass Spec: (M-Cl+H) calc m/z: 568.06654, expt m/z: 568.06902

EA: Expected: C – 45.81, H – 2.51, N – 6.97. Found C – 45.36, H – 2.36, N – 6.64

Synthesis of [Cp*$_2$Co] [Re(AbP)(CO)$_3$]$_2$, 2

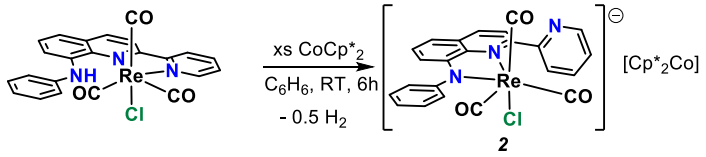

In an argon filled glovebox, 41 mg (1.2e-4 mol, 3 eq.) Cp*$_2$Co was added to a rapidly stirring suspension of **1** (25 mg, 4.14e-5 mol) in 10 mL anhydrous benzene in one portion. The colour slowly changed over time with formation of a purple precipitate. After 6 hours, the precipitate was filtered off with a glass fritted funnel and washed with copious amounts of C_6H_6 to remove unreacted **1** and Cp*$_2$Co. The purple solid was then washed wit h pentane and dried under reduced pressure to yield **2**. Final yield = 24 mg, 89%. The solid can be recrystallized from layered DCM:pentane.

^{1}H NMR (500 MHz, CD_2Cl_2) δ 8.72 (d, *J* = 4.8 Hz, 1H), 8.06 (d, *J* = 8.6 Hz, 1H), 8.00 (d, *J* = 6.6 Hz, 1H), 7.83 (t, *J* = 7.7 Hz, 1H), 7.49 (d, *J* = 8.4 Hz, 1H), 7.43 – 7.34 (m, 4H), 7.26 (t, *J* = 7.7 Hz, 1H), 7.19 (d, *J* = 7.0 Hz, 1H), 7.08 (t, *J* = 7.9 Hz, 1H), 7.02 (t, *J* = 6.5 Hz, 1H), 6.52 (d, *J* = 7.1 Hz, 1H), 6.44 (d, *J* = 8.3 Hz, 1H), 1.72 (s, 30H).

^{13}C NMR could not be obtained. Combination of poor solubility in solvents and the decomposition of **2** into **4** (which is accelerated in some solvents such as ACN) prevented accurate ^{13}C analysis within reasonable timescales.

IR (KBr pellet): ν(CO) = 1996, 1884, 1855

UV-Vis$_{DMF}$: λ = 429, 554 nm

EA: Expected: C – 55.45, H – 4.76, N – 4.51. Found C – 55.11, H – 4.27, N – 4.88

*Experiment to detect and quantify H2 production from the synthesis of **2***

Into a 25 mL 2-neck round bottom flask equipped with a Kontes tap, a Teflon coated stirbar and a rubber septa (total volume 29.3452 ± 0.002 mL with adaptors etc.) was added 25 mg **1**. 41 mg Cp^*_2Co (3 eq,) dissolved in 7 mL anhydrous C_6H_6 was transferred via syringe under an Ar atmosphere. 50 uL headspace aliquots were taken for GC-PDHID analysis and quantification. The experiment was repeated in triplicate to yield 0.24 eq ±0.09 H2.

Leaks in the reaction flask joints/septa, H· consumption by adventitious acceptors (H_2O/DCM/ligand decomposition etc), or H_2 remaining dissolved in solution could explain this low quantified yield on such small scales

Procedure for the Chemical Reduction of 1 with 2.2 eq. KC_8

In an argon filled glovebox, a 20 mL scintillation vial was charged with 20 mg **1** (3.3e-5 mol) and 5 mL anhydrous THF. 5 mg (1.1 eq.) freshly prepared KC_8 was slowly added at room temperature. The suspension was allowed to stir for 1h before filtration through a 0.2 um PTFE syringe filter to yield a deep purple solution. The solvent was removed under vacuum and the solid taken up in C_6D_6 for NMR analysis (Fig S**). The NMR sample was removed from the J-Young tube and layered with pentane, from which grew crystals of the dearomatized complex reported in the manuscript.

Synthesis of $[Re(AbP)(CO)_3]_2$, 4

4

In an argon filled glovebox, 45 mg **1** (7.46e-5 mol) was taken up in 5 mL anhydrous THF. A solution of 17 mg (8.52e-5 mol, 1.2 eq.) KHMDS was made up in 1 mL anhydrous THF and added dropwise to the rapidly stirring **1** solution with an immediate colour change to dark blue. The solution was stirred for 1 hour before filtering through a 0.2 um PTFE syringe filter using extra THF to wash though. The solvent was removed under reduced pressure and the dark blue solid was triturated with copious amounts of

anhydrous hexanes to remove excess KHMDS. The solid was recrystallized from layering DCM and pentane. Final yield = 0.038 g, 92%. While the complex was found to be air stable, it was stored and manipulated for further reactivity entirely within an argon filled glovebox.

^{1}H NMR (500 MHz, CD2Cl2) δ 9.58 (d, J = 6.0 Hz, 1H), 8.15 (d, J = 8.5 Hz, 1H), 7.83 (td, J = 7.6, 1.6 Hz, 1H), 7.49 – 7.31 (m, 7H), 7.13 (ddd, J = 8.5, 6.8, 1.9 Hz, 1H), 7.05 (dd, J = 8.2, 1.1 Hz, 1H), 6.85 – 6.80 (d, 1H, J = 7.6 Hz),

13C NMR (126 MHz, CD2Cl2) δ 198.97, 195.63, 192.66, 164.00, 162.20, 159.01, 158.83, 155.65, 151.84, 144.47, 138.75, 138.45, 131.90, 130.77, 129.87, 129.15, 127.46, 126.42, 126.14, 124.11, 123.48, 112.56, 110.20.

IR (KBr pellet): v(CO) = 2008, 1919, 1872

UV-Vis$_{DMSO}$: λ = 410, 580 nm

EA: Expected: C – 48.76, H – 2.49, N – 7.42. Found C – 49.03, H – 3.01, N – 6.98

Synthesis of [Re(AbP)(CO)$_3$DMAP], 5

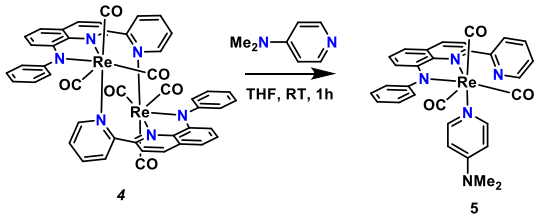

In an argon filled glovebox, to a rapidly stirring solution of **4** (57 mg, 5.03e-5 mol) in ~5 mL anhydrous THF, 12 mg (1.0e-4 mol, 2 eq.) of 4-dimethylaminopyridine (DMAP) was added in one portion with immediate colour change to a vibrant blue. The solution was stirred for 1 hour before filtering through a 0.2 um PTFE syringe filter. The solvent was removed under reduced pressure and the blue solid was triturated with copious amounts of pentane to remove excess DMAP. The solid was recrystallized from layered THF and pentane. Final yield = 63 mg, 95%. While the complex was found to be air stable, it was stored and manipulated for further reactivity entirely within an argon filled glovebox.

^{1}H NMR (500 MHz, CD2Cl2) δ 8.74 (d, J = 4.8 Hz, 1H), 8.12 (d, J = 8.5 Hz, 1H), 7.89 (d, J = 7.2 Hz, 1H), 7.86 (td, J = 7.7, 1.8 Hz, 1H), 7.56 – 7.47 (m, 3H), 7.43 – 7.36 (m, 4H), 7.13 (t, J = 8.0 Hz, 1H), 7.07 (tt, J = 7.0, 1.6 Hz, 1H), 6.80 (dd, J = 8.3, 1.1 Hz, 1H), 6.61 (d, J = 7.6 Hz, 1H), 6.27 (d, J = 7.3 Hz, 1H), 2.91 (s, 6H)

13C NMR (126 MHz, CD2Cl2) δ 197.78, 194.67, 159.13, 157.75, 156.61, 154.57, 153.64, 150.63, 148.22, 143.58, 137.44, 135.28, 130.29, 128.77, 128.58, 127.71, 126.05, 125.36, 123.52, 122.22, 121.96, 108.90, 106.71, 106.48, 67.17, 53.29, 53.08, 52.95, 52.86, 52.64, 52.43, 38.30.

IR (KBr pellet): v(CO) = 2003, 1892, 1875

UV-Vis$_{DMF}$: λ_{max} = 585 nm

EA: Expected: C – 52.32, H – 3.51, N – 10.17. Found C – 51.99, H – 3.68, N – 10.56

Synthesis of A^{Me}bP, iii

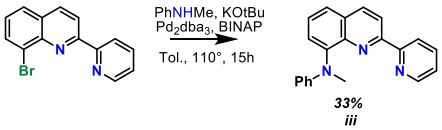

0.500 g **i** (1 eq., 0.0017 mol), 0.056 g Pd_2dba_3 (3%, 0.03 eq, 6. 1e-5 mol), 0.076 g rac-BINAP (7%, 0.07 eq, 12e-4 mol), 0.235 KOtBu (1.2 eq, 0.0021mol), 0.195 g N-methyl aniline (1.2 eq. 0.021 mol) were combined in a thick-walled glass bomb along with 15 mL dry toluene. The solution was heated to 110°C overnight. Curiously the compound was found to decompose on silica (confirmed via 2D TLC) despite the confirmed stability of **ii** to the same conditions. After cooling to room temp, the reaction solution was diluted with $CHCl_3$ and washed with 3x 50mL portions of DI water. The organic phase was then extracted with 5x 50mL, pH = 1 water. The pink aqueous phase was rebasified to pH 13 and extracted with 3x 50 mL portions of $CHCl_3$. The organic phase was washed with 1x 50 mL brine and dried with Na_2SO_4, and the solvent removed under reduced pressure to yield a bright yellow powder. This was then recrystallized from hot MeOH twice before metalation. Final yield = 0.13 g, 33%

^{1}H NMR (500 MHz, $CDCl_3$) δ 8.65 (ddd, *J* = 4.8, 1.9, 0.9 Hz, 1H), 8.53 (d, *J* = 8.6 Hz, 1H), 8.28 (d, *J* = 8.6 Hz, 1H), 7.91 (dt, *J* = 7.9, 1.1 Hz, 1H), 7.66 (td, *J* = 7.8, 1.7 Hz, 2H), 7.61 (dd, *J* = 7.5, 1.4 Hz, 1H), 7.54 (t, *J* = 7.7 Hz, 1H), 7.29 – 7.25 (m, 1H), 7.24 – 7.18 (m, 2H), 6.92 – 6.86 (m, 2H), 6.85 – 6.79 (m, 1H), 3.61 (s, 3H).

^{13}C NMR (126 MHz, CDCl3) δ 156.63, 155.42, 152.93, 148.47, 147.39, 141.30, 140.06, 137.21, 136.49, 128.88, 128.48, 128.30, 127.02, 124.74, 124.40, 121.93, 121.69, 120.13, 119.03, 115.95, 107.46, 76.73, 76.47, 76.22, 20.82.

UV-Vis$_{DMF}$: λ_{max} = 410 nm (522 $M^{-1}cm^{-1}$)

EA: Expected: C – 81.00, H – 5.50, N – 13.49. Found C –81.29, H – 6.11, N – 12.94

Synthesis of Re(AbP)(CO)$_3$Cl, 6

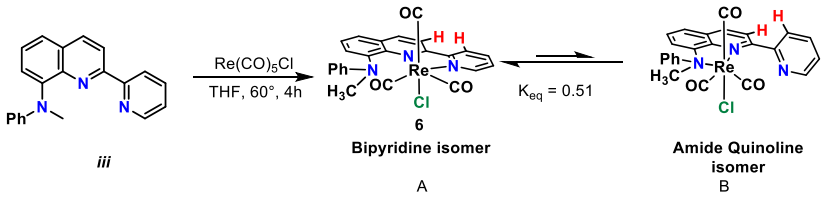

In an argon filled glovebox, 200 mg **iii** (6.4e-4 mol, 1.0 eq) and 220 mg $Re(CO)_5Cl$ (6.1e-4 mol, 0.95 eq) were combined with 30 mL anhydrous THF in a 100 mL Schlenk flask with a teflon Kontes tap. The solution was heated to reflux for 4 hours before cooling to room temperature and opening to atmosphere. The solvent was removed under reduced pressure and the purple solid was triturated with hexane to remove excess **iii**. Final yield = 0.365 g, 100% based on Re starting material used.

^{1}H NMR (500 MHz, $CDCl_3$) δ 9.16 (d, *J* = 5.3 Hz, 0.5H), 8.99 (dd, *J* = 5.5, 1.6 Hz, 1H), 8.57 (d, *J* = 8.5 Hz, 1H), 8.25 (d, *J* = 8.1 Hz, 1H), 8.18 (d, *J* = 8.1 Hz, 1H), 8.16 – 7.97 (m, 4H), 7.87 – 7.75 (m, 3H), 7.58 – 7.52 (m, 1H), 7.50 (d, *J* = 8.2 Hz, 1H), 7.44 (ddd, *J* = 7.3, 4.4, 1.3 Hz, 1H), 7.42 – 7.34 (m, 1H), 6.91 – 6.84 (m, 2H), 6.63 (t, *J* = 7.2 Hz, 1H), 6.02 (d, *J* = 8.3 Hz, 2H), 3.90 (s, 3H), 2.96 (s, 2H).

^{13}C NMR (126 MHz, $CDCl_3$) δ 196.73, 196.29, 196.01, 195.09, 190.69, 189.79, 159.50, 159.42, 157.53, 157.04, 152.72, 152.56, 148.54, 147.84, 146.42, 146.18, 145.42, 144.49, 141.59, 141.17, 138.28, 138.17, 130.97, 129.62, 129.09, 128.65, 128.47, 128.07, 128.03, 127.84, 127.65, 127.60, 126.28, 125.37, 125.30, 124.49, 124.30, 124.25, 123.81, 123.55, 122.98, 121.98, 120.60, 119.12, 118.89, 118.77, 117.99, 115.73, 115.17, 110.96, 76.70, 76.65, 76.45, 76.19, 42.15, 42.08

IR_{KBr} : v(CO) = 2016, 1919, 1872

IR $soln_{DMF}$: v(CO) = 2022, 1918, 1893

UV-Vis_{DMSO}: λ_{max} = 432, 517 (shoulder) nm

ESI-Mass Spec: (M-Cl+H) calc m/z: 568.06654, expt m/z: 568.06902

EA: Expected: C – 46.71, H – 2.78, N – 6.81. Found C – 46.69, H – 2.88 , N –6.29

NMR Spectra

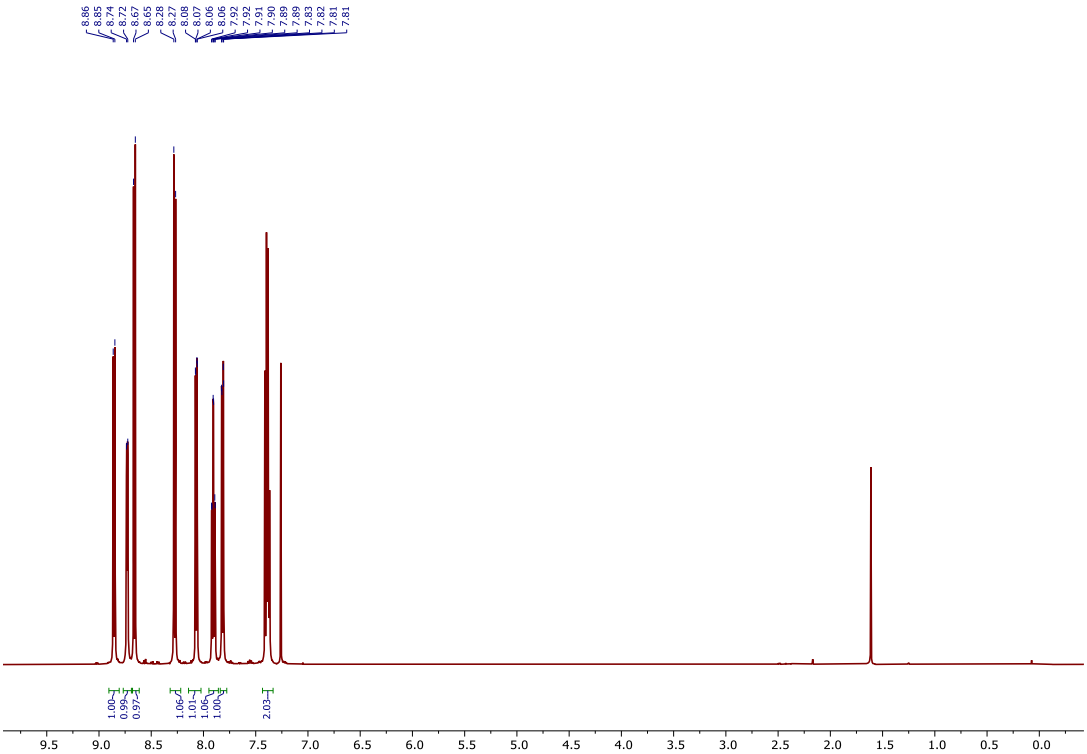

Fig S1: ^{1}H NMR spectrum of **i**, $CDCl_3$

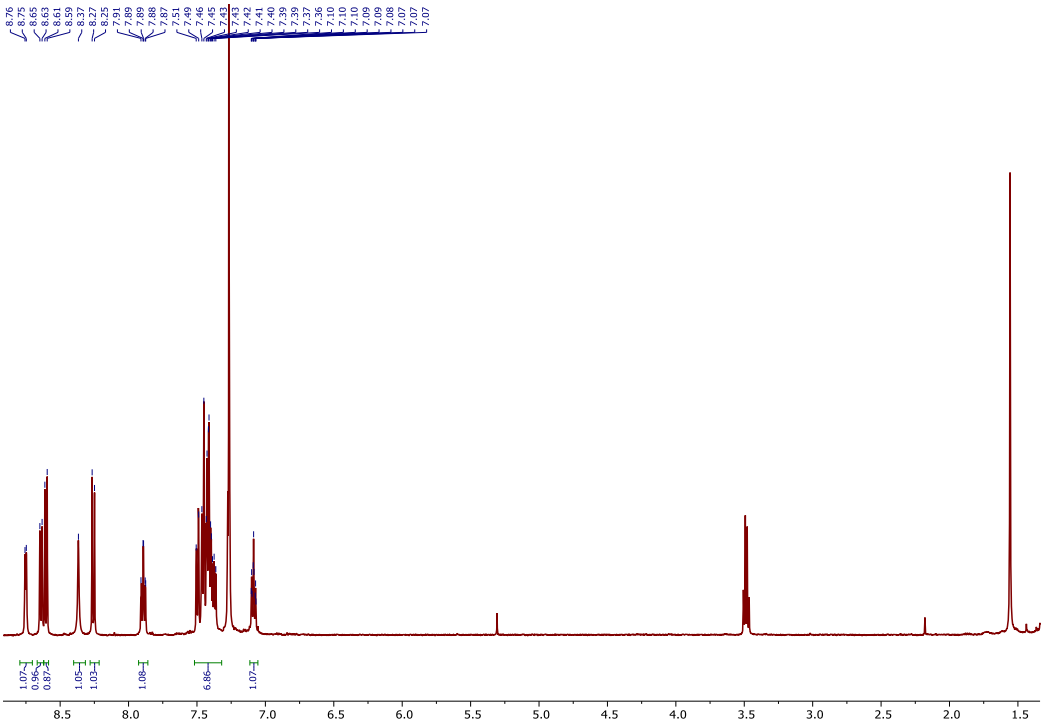

Fig S2: ^{1}H NMR spectrum of **iii,** $CDCl_3$

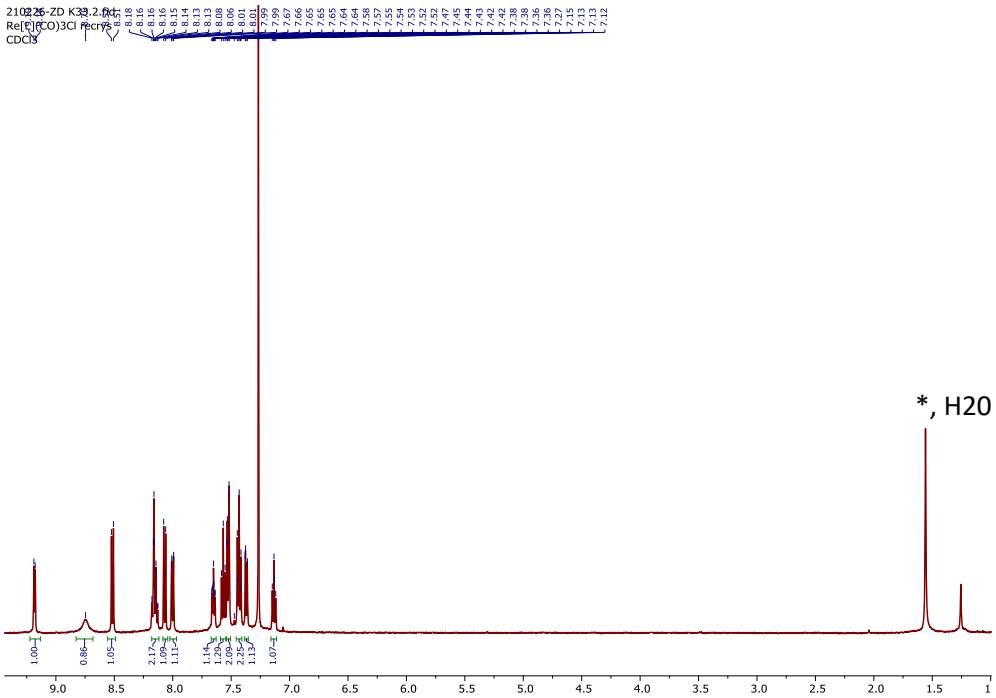

Figure S3: ^{1}H NMR spectrum of **1,** $CDCl_3$. Asterisks denote known impurities

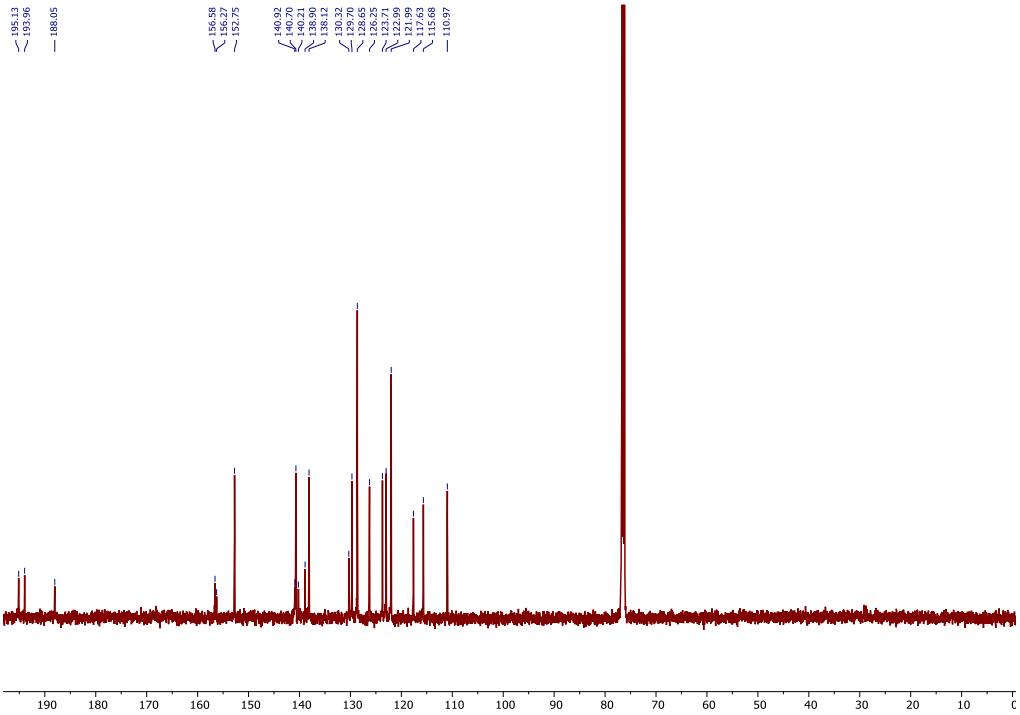

Fig S4: ^{13}C UDEFT NMR spectrum of **1,** $CDCl_3$

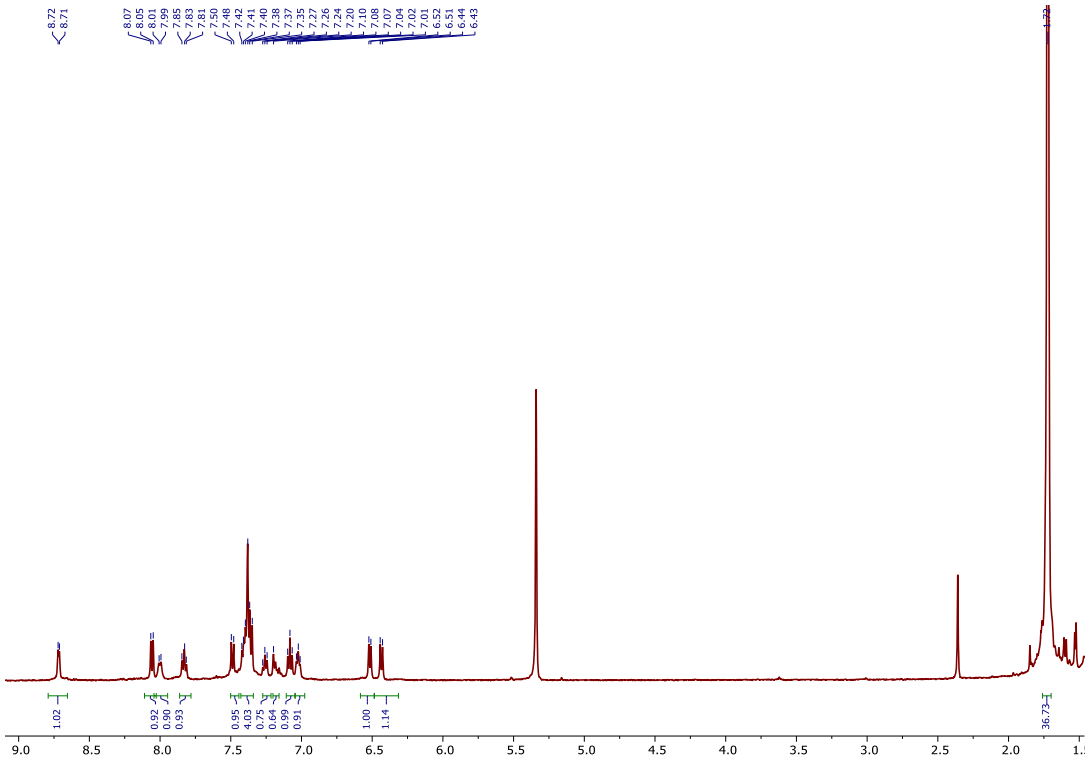

Figure S5: ^{1}H NMR spectrum of **2,** CD_2Cl2

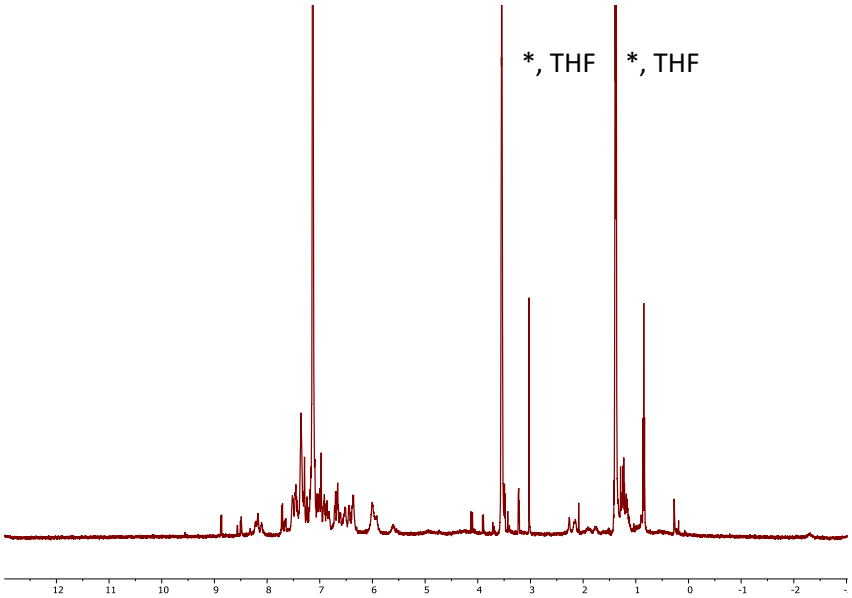

Fig S6: ^{1}H NMR in C_6D_6 of the reaction of **1** with 2.2 eq. of KC_8 after workup. Asterisks denote known impurities

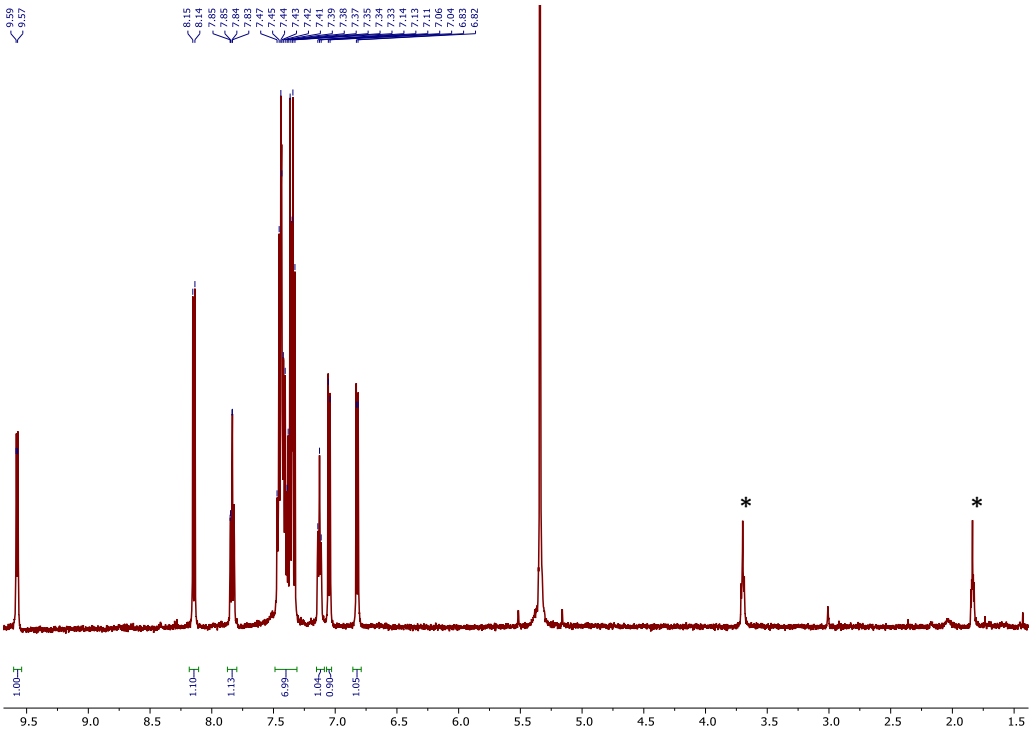

Fig S7: 1H NMR of **4** in CD_2Cl_2. Asterisks denote known impurities (THF)

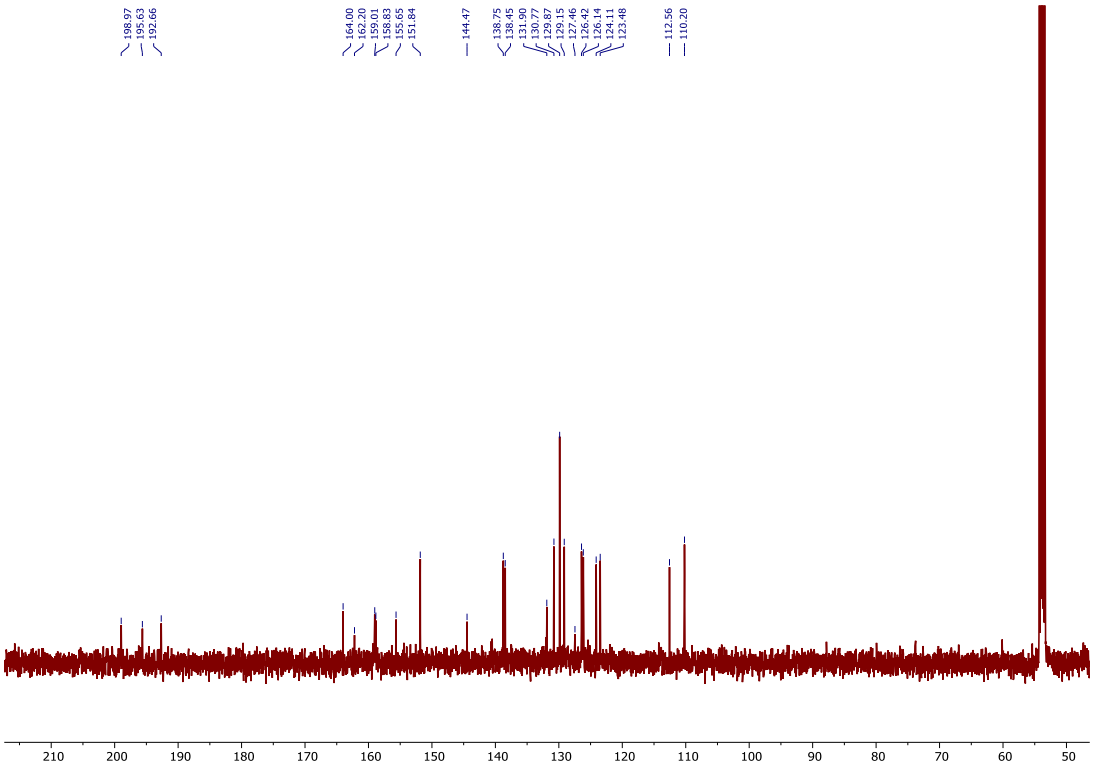

Fig S8: ^{13}C UDEFT NMR of **4** in CD_2Cl_2

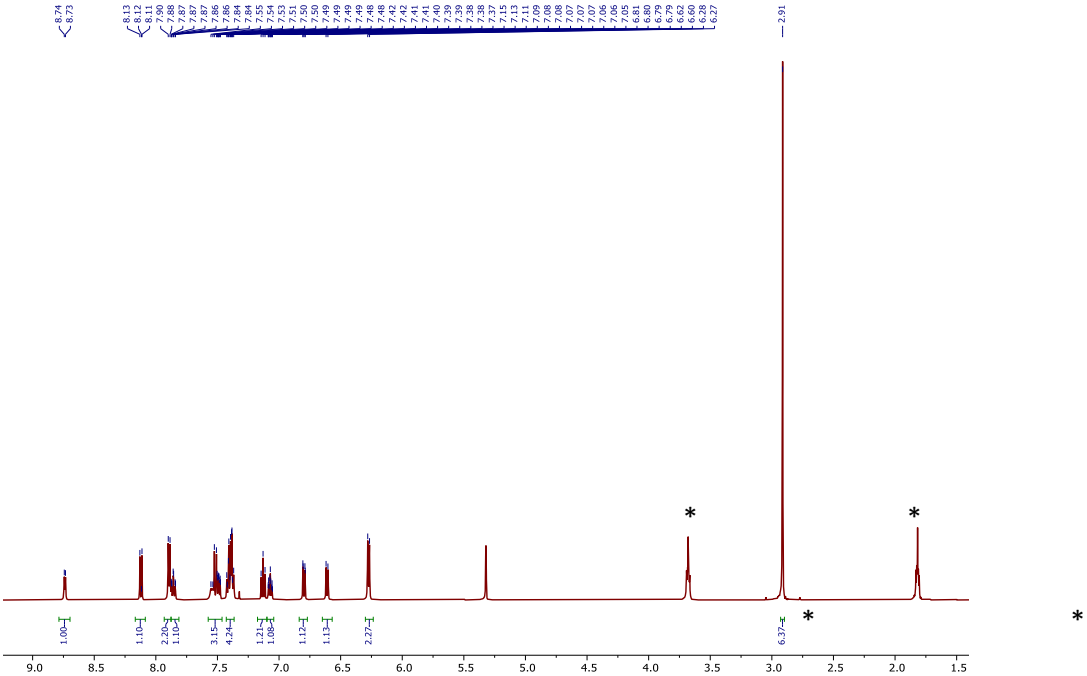

Fig S9: 1H NMR of ReDMAP, **5** in CD_2Cl_2. Asterisks denote known solvent impurities (THF)

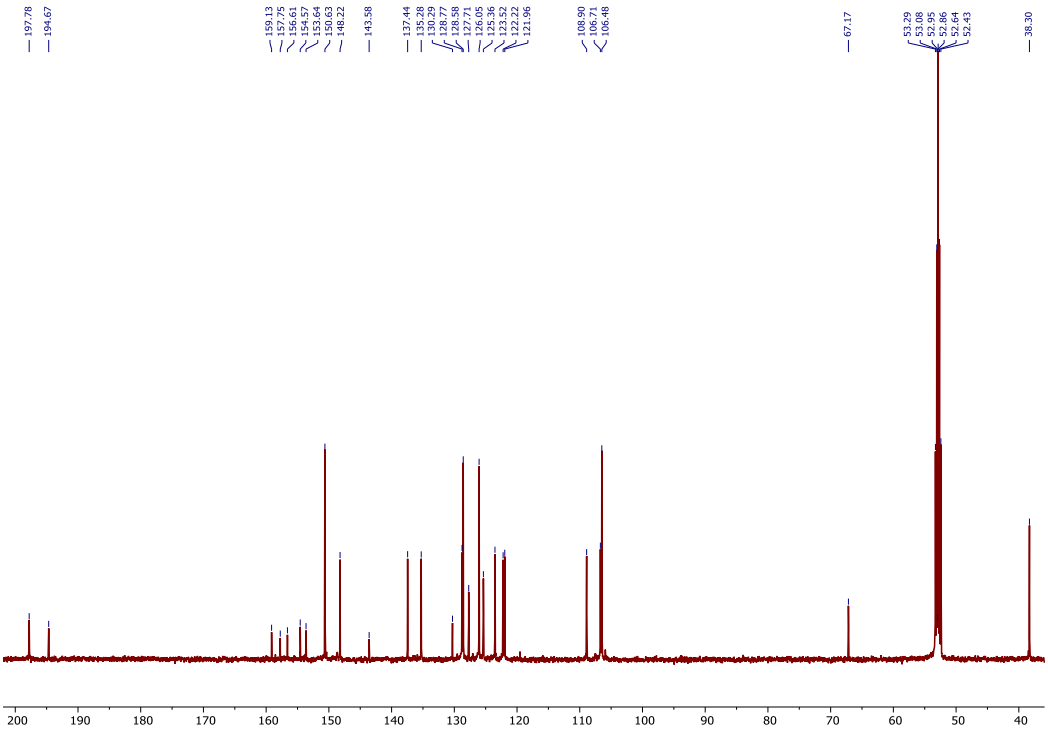

Fig S10: 13C UDEFT NMR of ReDMAP, **5** in CD_2Cl_2

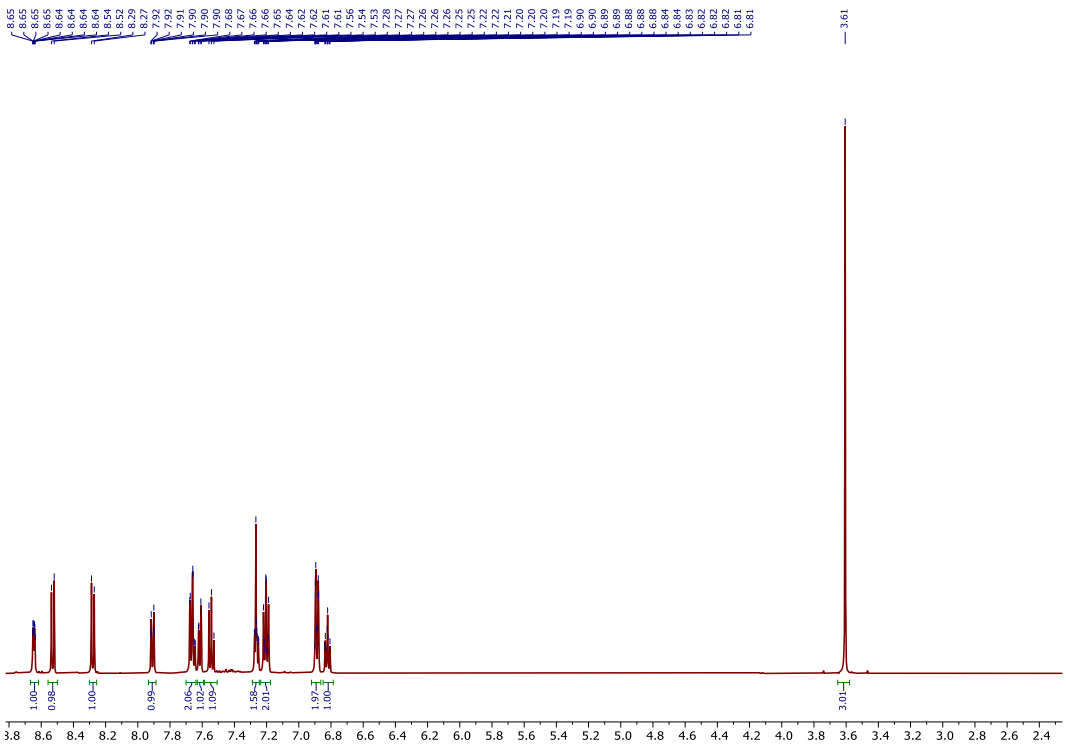

Fig S11: 1H NMR of **iii** in $CDCl_3$

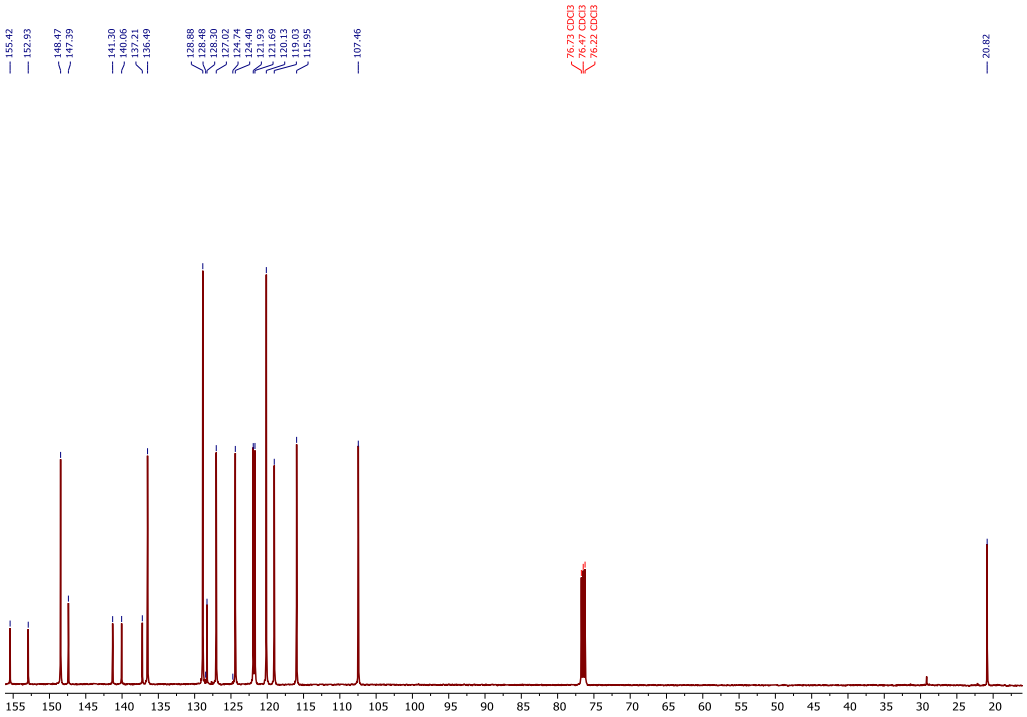

Fig S12: 13C UDEFT NMR of **iii** in $CDCl_3$

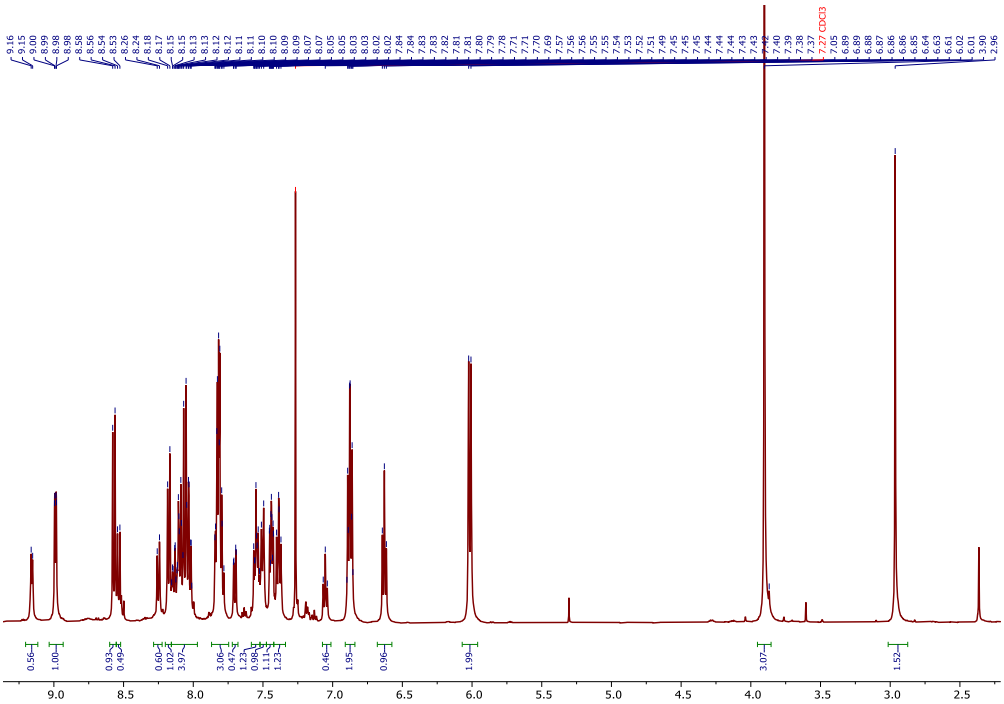

Fig S13: 1H NMR of**6** in $CDCl_3$ showing both species in solution in a 2:1 ratio

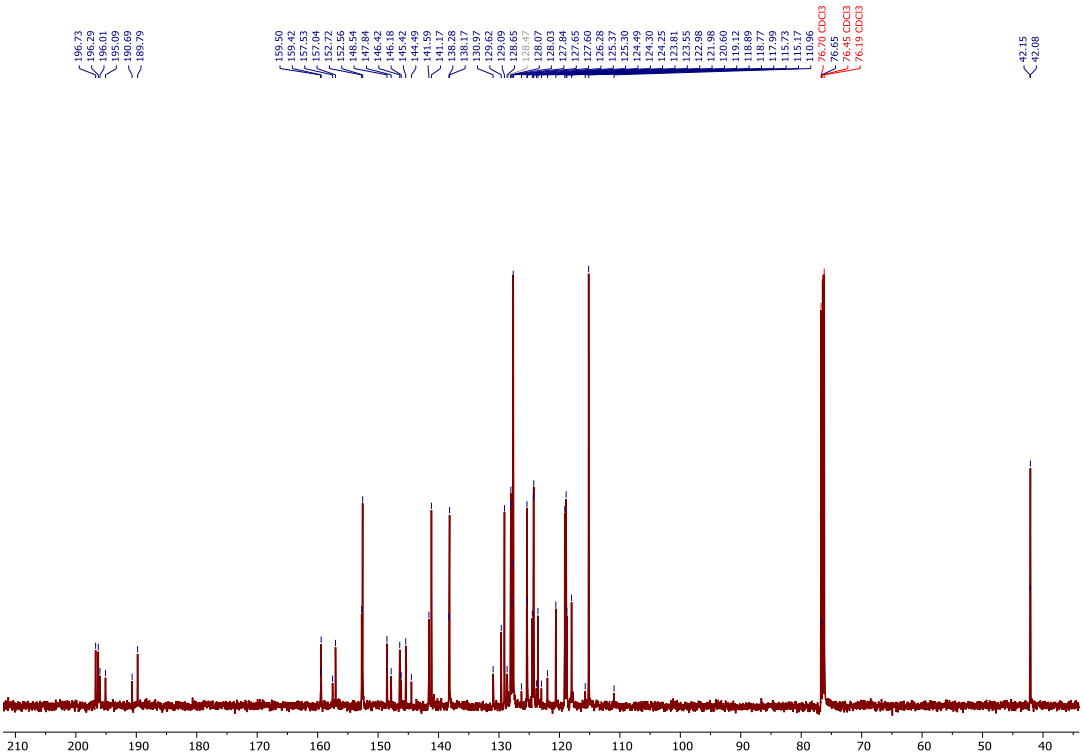

Fig S14: 13C UDEFT NMR of **6** in $CDCl_3$ showing both species in solution.

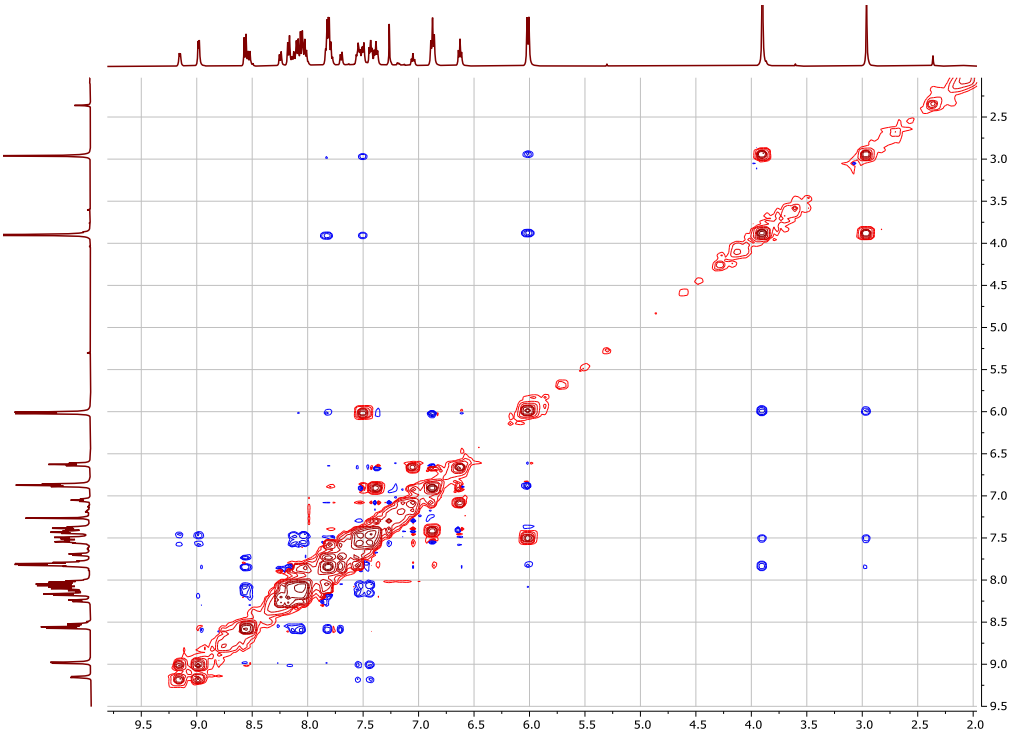

Fig S15: NOESY/EXSY NMR of **6** in degassed $CDCl_3$. Blue cross peaks are NOE signals, red are exchange signals. D8 = 0.75s. COSY-like symmetrisation applied to increase S/N

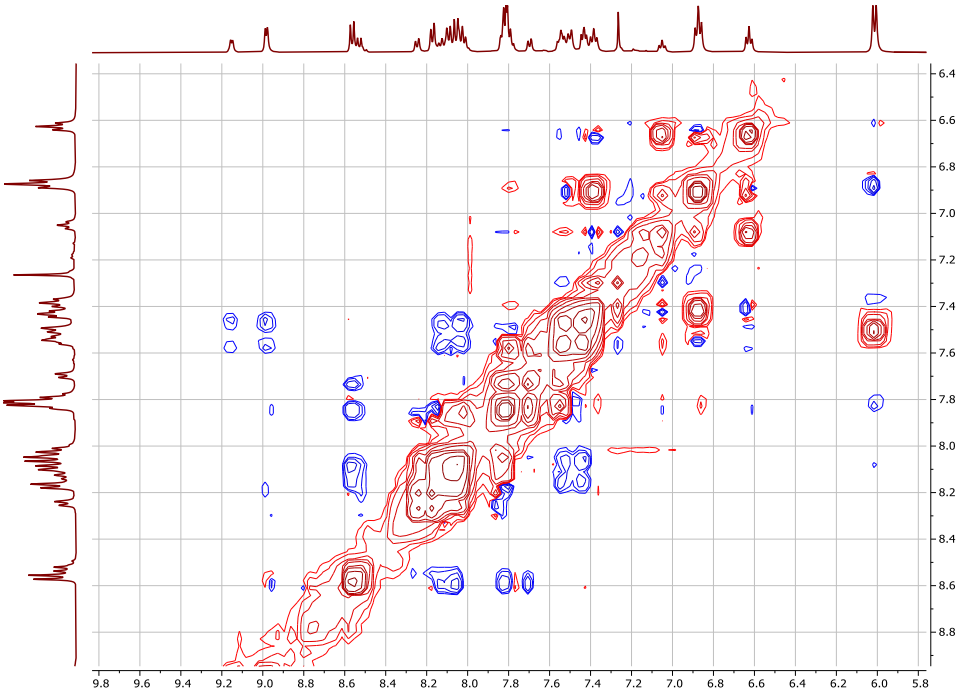

Fig S16: Expansion of aromatic region NOESY/EXSY NMR of **6** in degassed $CDCl_3$. Blue cross peaks are NOE signals, red are exchange signals. D8 = 0.75s. COSY-like symmetrisation applied to increase S/N.

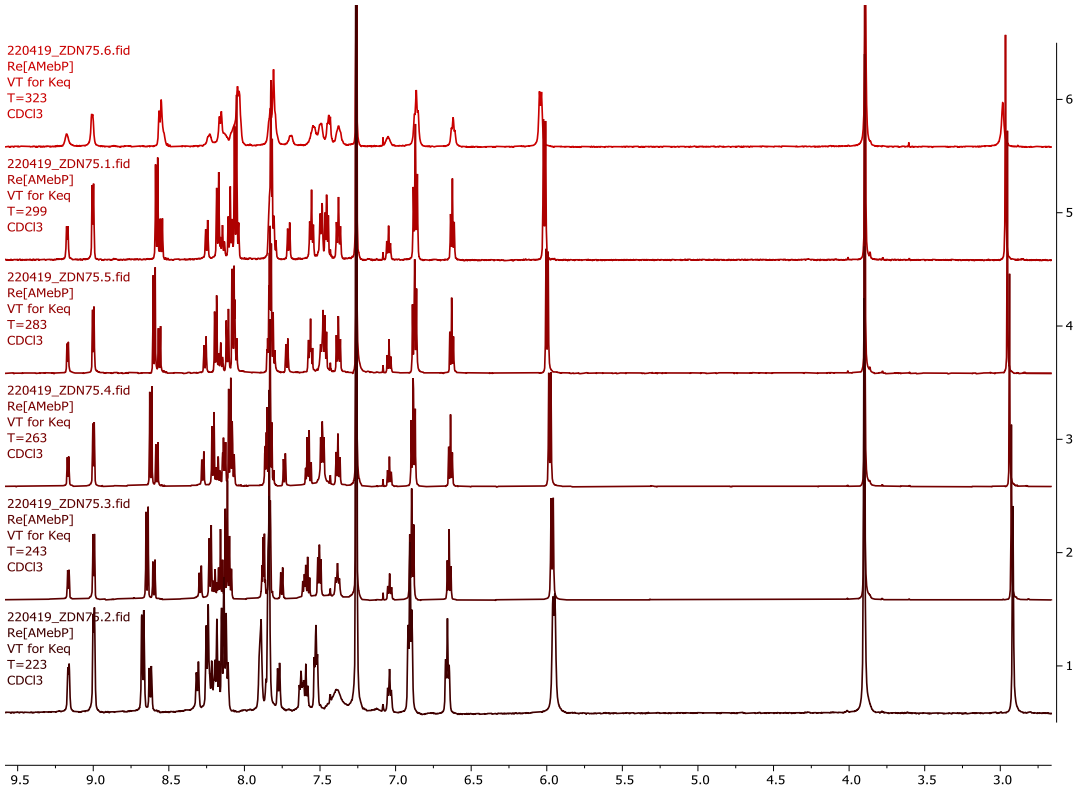

Fig S17: Attempts at V'ant Hoff analysis of **6** in $CDCl_3$. Note the very low change in integrals with changing temperature.

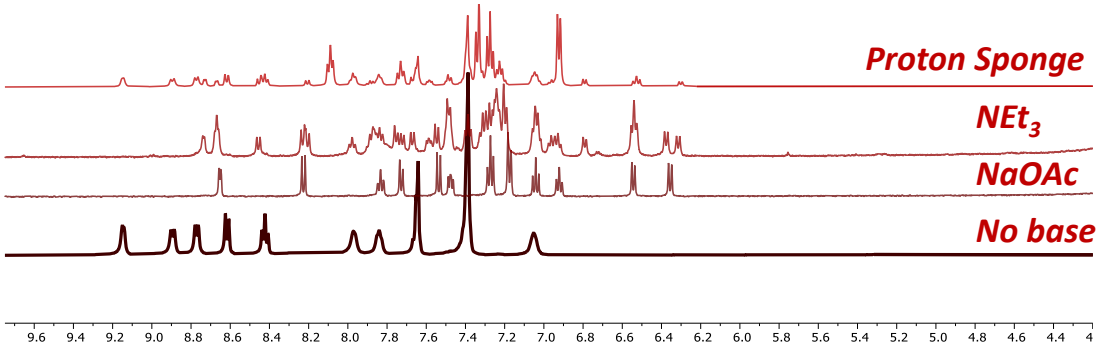

Fig S18: NMR experiments with bases of various basicity to determine pKa of complex **1** in d_6 DMSO, 500 Mhz. Simply comparing the spectra between without a base vs with base added shows at what pKa **1**is deprotonated.

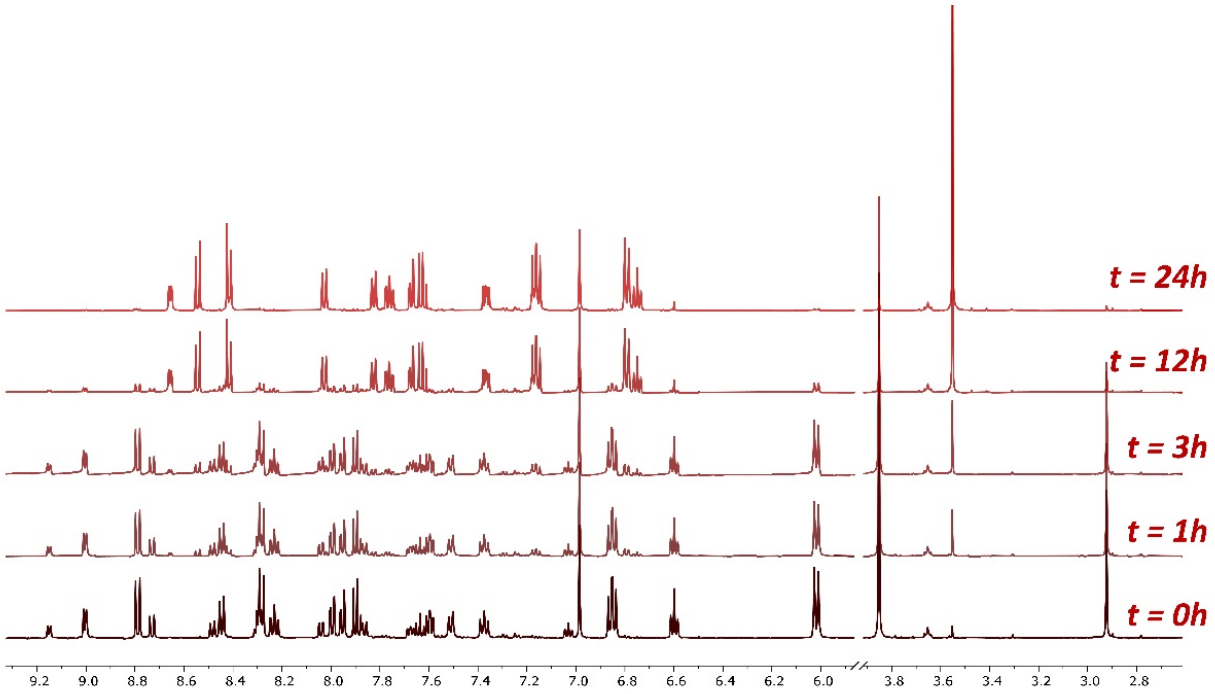

Fig S19: The decomposition of **6 a**t room temperature in anhydrous and degassed CD3CN in the dark, over time. Moderate heating was found to greatly accelerate this decomposition with total demetallation of the complex observed after 30 minutes at 50 °C. Other polar solvents do not seem to have the same effect; no decomposition was observed when **6** was exposed to DMF, THF or MeOH.

Spectroelectrochemistry Data

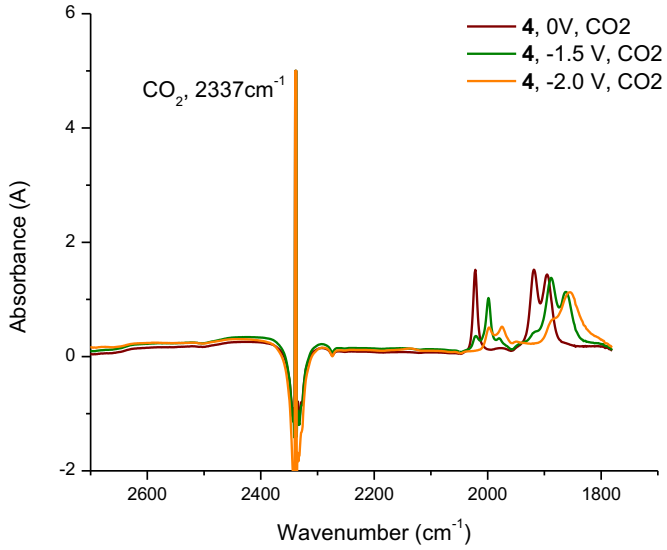

Figure S20: Spectroelectrochemical spectra for **1** with CO_2 sparged DMF. 0.3M $TBAPF_6$, Pt mesh, CE: Pt wire, RE: Ag wire

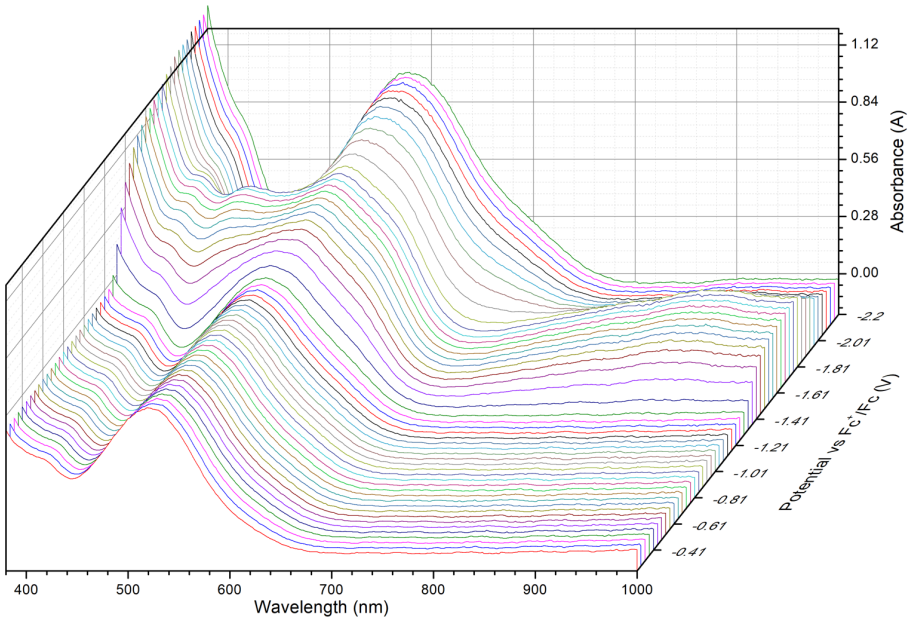

Fig S21: UV-Vis SEC of complex **1** in DMF, 0.3 M TBAPF6. WE: Pt mesh, CE: Pt wire, RE: Ag wire

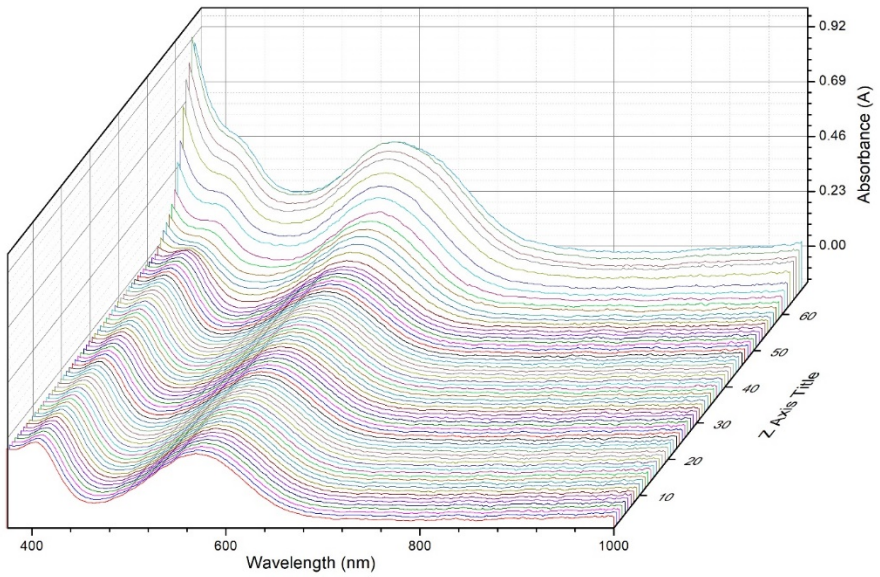

Fig S22**:** UV-Vis SEC of complex **4** in DMF, 0.3 M TBAPF6. WE: Pt mesh, CE: Pt wire, RE: Ag wire

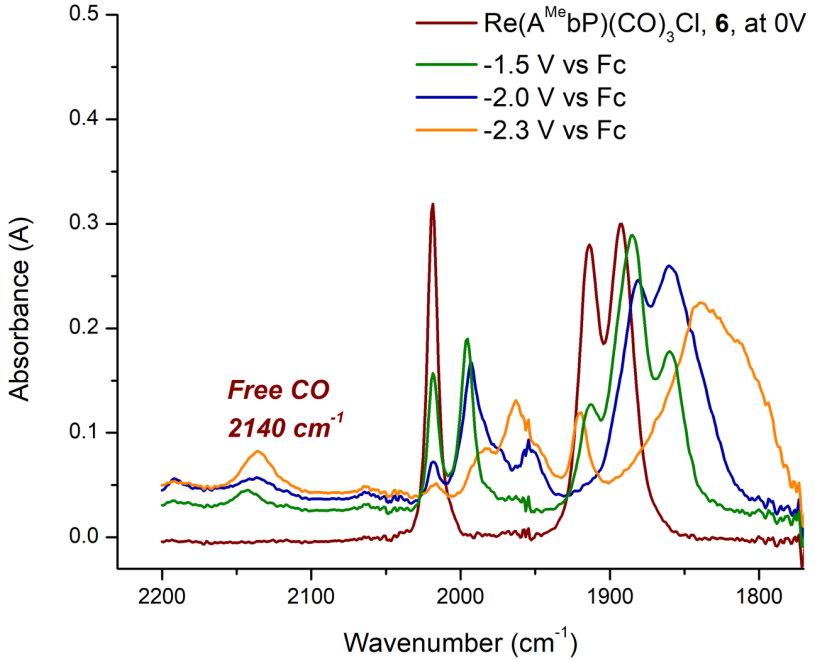

Fig S23: IR-SEC of **6** with 0.3 M $TBAPF_6$ in DMF under Ar. Pt mesh WE, Pt wire CE, Ag wire RE

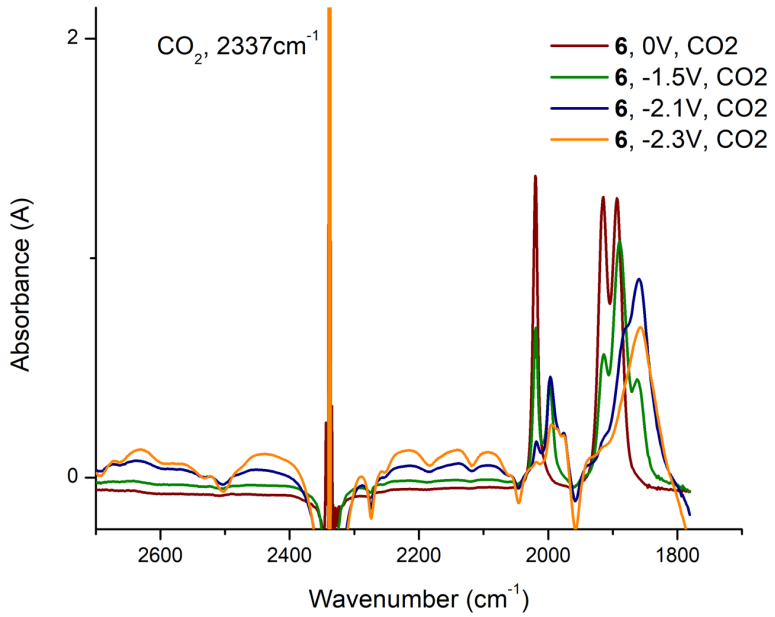

Fig S24: IR-SEC of **6** in 0.3 M $TBAPF_6$ DMF with CO_2 sparged DMF. Pt mesh WE, Pt wire CE, Ag wire RE

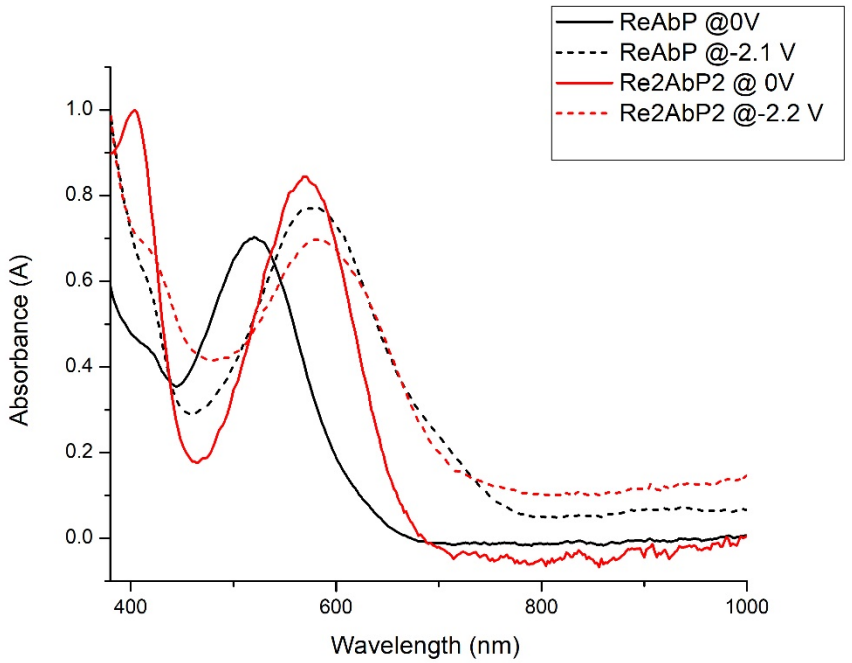

Fig S25: Comparing the start and end points of UV-Vis SEC experiments between **1** and **5** in DMF, 0.3M TBAPF6.

IR Spectra

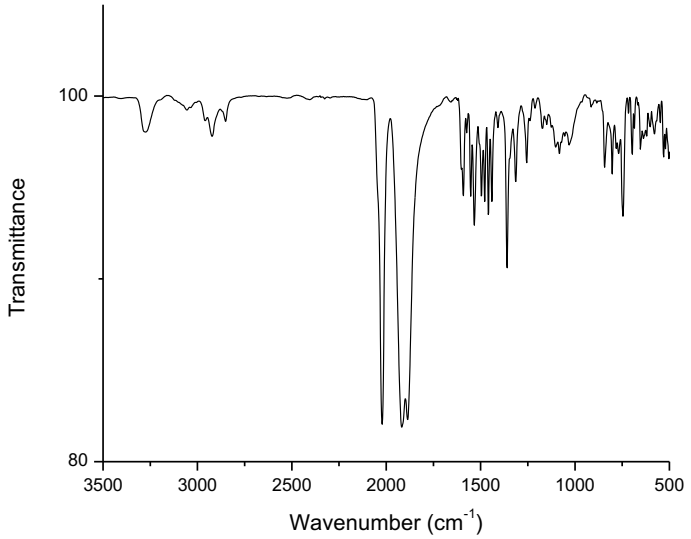

Fig S26: IR spectrum of **1**collected as a KBr pellet

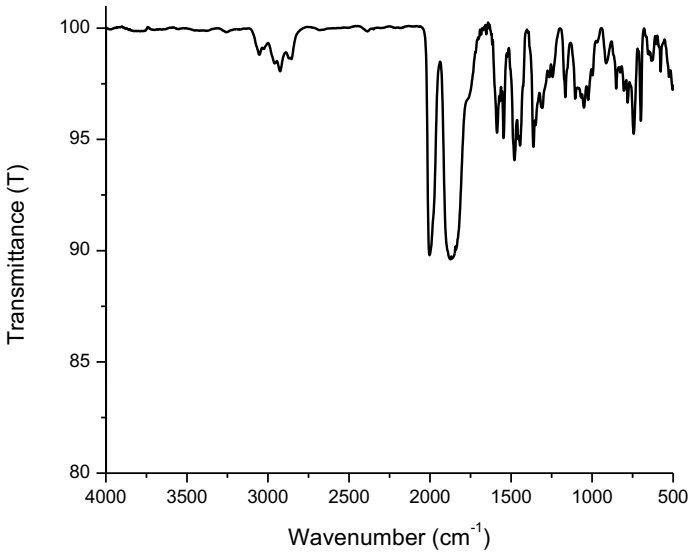

Fig S27: IR spectrum of **2** collected as a KBr pellet

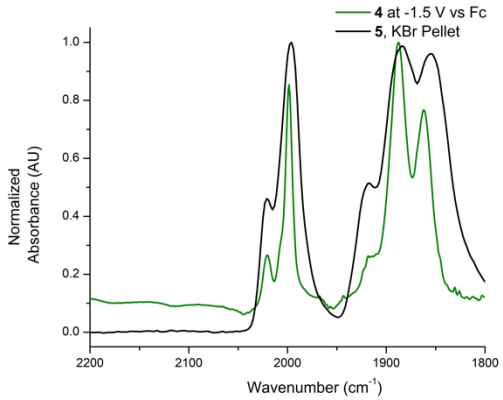

Fig S28: Overlay of KBr pellet IR spectrum of **2** with SEC data of **1** in DMF at -1.5 V vs Fc

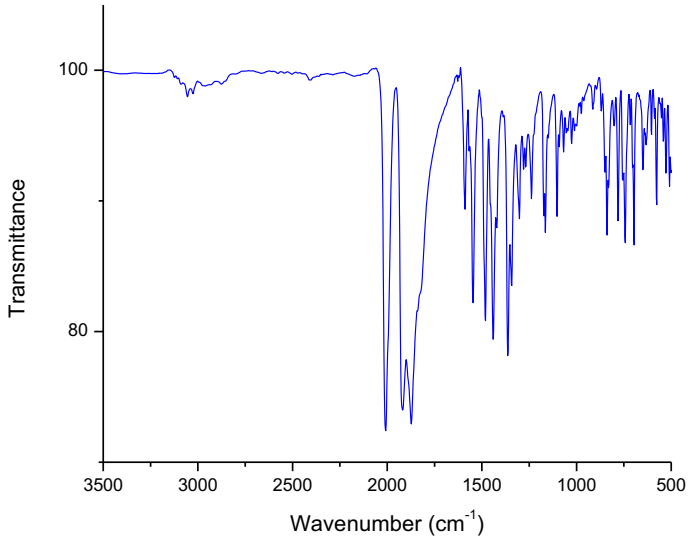

Fig S29: IR spectrum of **4** collected as a KBr pellet

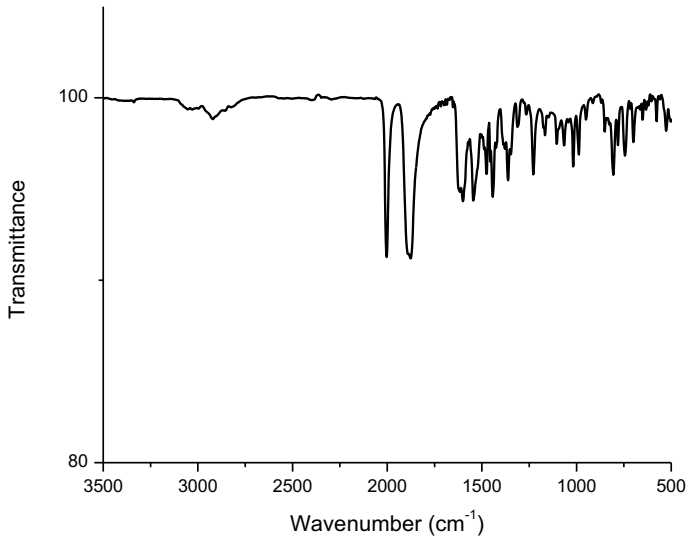

Fig S30: IR spectrum of **5** collected as a KBr pellet

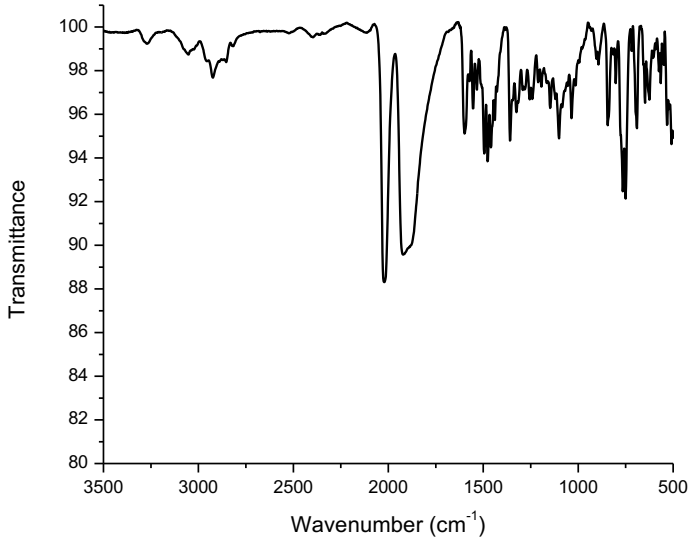

Fig S31: IR spectrum of **6** collected as a KBr pellet

Electrochemistry

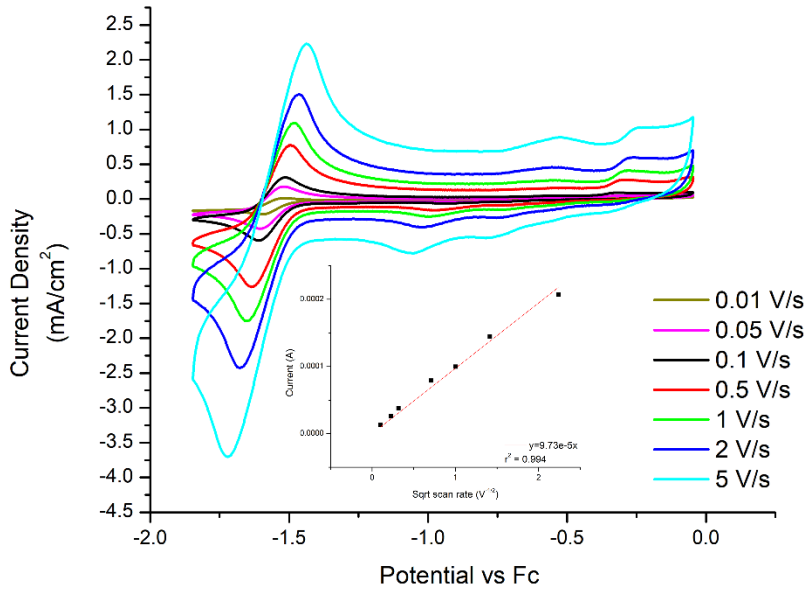

Fig S32: Different scan rates for the first reductive wave of complex **1**. CVs taken in DMF with GC disk WE, Pt mesh CE and Ag/AgCl reference electrode. Inset is square root of scan rate vs current

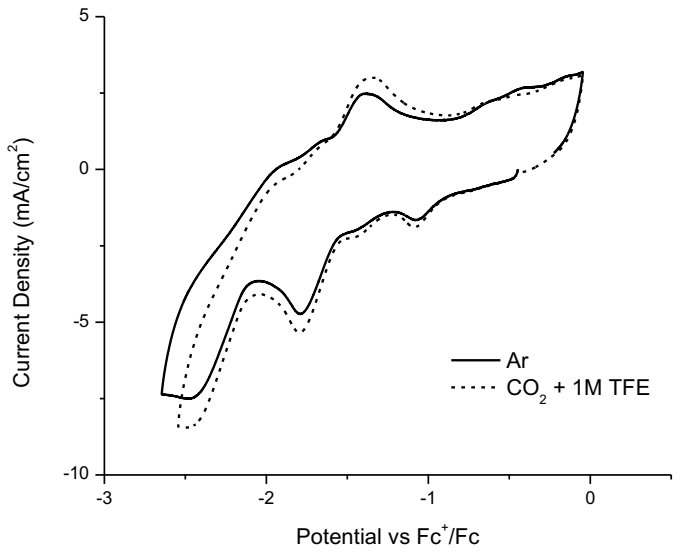

Fig S33: CV of **1** at 13 V/s under Ar and CO_2 with 1M TFE. GC WE, Pt mesh CE, and Ag/AgCl pseudoreference.

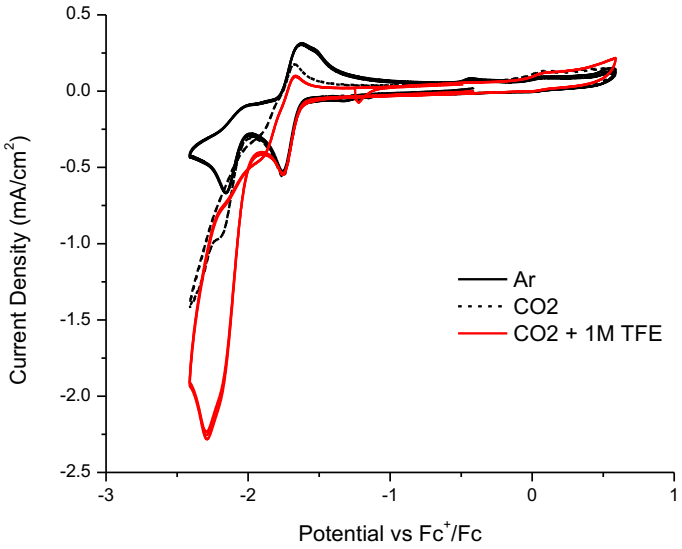

Fig S34: Re(bpy)(CO)$_3$Cl CV at 0.1 V/s with GC WE, Pt mesh CE, and Ag/AgCl psedoreference electrodes. Under an atmosphereof CO_2

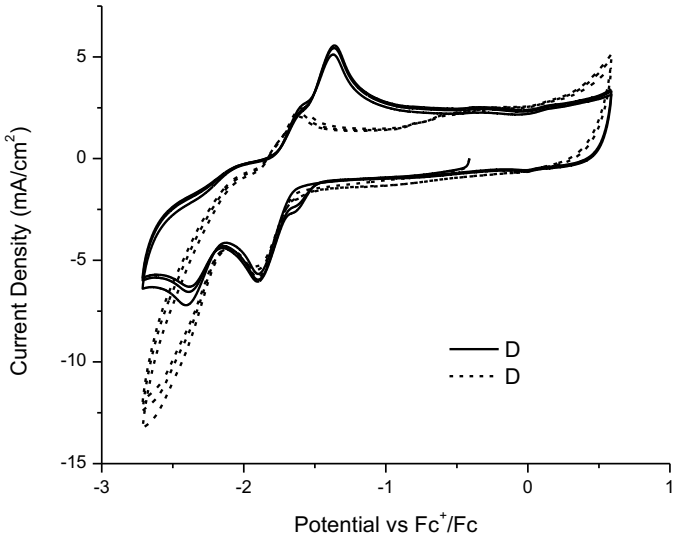

Fig S35: CV of Re(bpy)(CO)$_3$Cl at 15V/s in DMF. GC WE, Pt mesh CE and Ag/AgCl pseudoreference.

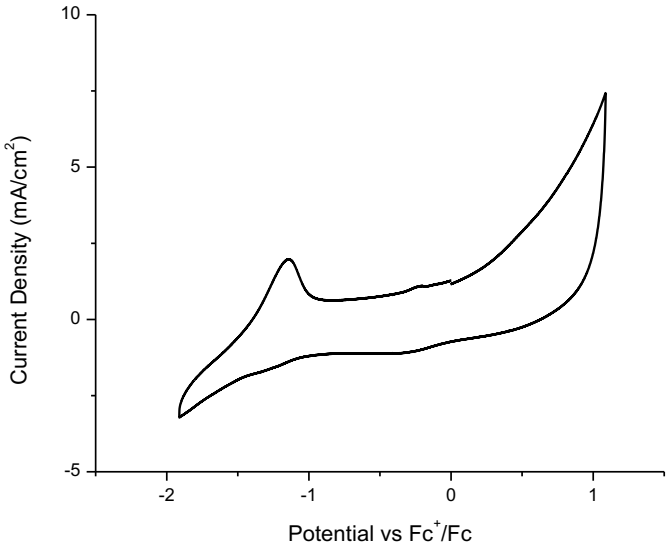

Fig S36: Representative rinse test from CPE experiments. The GC electrode used in the CPE was gently rinsed with clean solvent and immersed in 0.1M DMF. A CV was taken at 0.1 V/s with Pt mesh CE and Ag/AgCl pseudoreference

Table S2: Electrolysis results under different conditions.

Conditions	No Catalyst, DMF, 1M TFE, -2.0 V		1, DMF, 1 M TFE, -2.0 V [a]		1, DMF, 1M PhOH, -2.0 V [b]		1, DMF 1M H_2O, -2.0 V [b]		1, MeCN, 1M TFE, -2.0 V [b]		5, DMF, 1M TFE-2.2 V [b,]		6, DMF, 1M TFE, -2.0 V [c]		Post CPE electrode, DMF, 1M TFE, -2.0 V [b,d]	
Time	TON_{CO}	FE_{CO}	TON_{CO}	FE_{CO}	TON_{CO}	FE_{CO}	TON_{CO}	FE_{CO}	TON_{CO}	FE_{CO}	TON_{CO}	FE_{CO}	TON_{CO}	FE_{CO}	TON_{CO}	FE_{CO}
0.5	0	0	0.51 (± 0.16)	30.5 ((± 8)	n/a	n/a	n/a	n/a	n/a	n/a	0	0	0.087 (± 0.04)	17.49 (± 7.4)	0	0
1	0	0	1.2 (± 0.27)	49.8 (± 5)	0.17	19.0	1.4	41.2	0.6	22.1	0	0	0.21(± 0.00)	25.93(± 9.24)	0	0
1.5	0	0	2.1 (± 0.8)	80.9 (± 8)	n/a	n/a	n/a	n/a	n/a	n/a	0	0	0.32(± 0.023)	30.48 (± 7.38)	0	0
2	0	0	2.4 (± 0.27)	88.0 (± 12)	0.26	25.7	1.9	36.6	1.1	34.3	0	0	0.419(± 0.07)	32.6 (± 3.95)	0	0
3	0	0	3.6 (± 0.74)	88.0 (±11)	0.48	20.3	2.1	29.5	1.5	37.7	0	0	0.614(± 0.101)	37.46 (± 3.32)	0	0
4	0	0	4.1 (± 0.6)	87.5 (± 11)	0.53	18.3	2.6	30.1	1.8	45.9	0	0	0.776(± 0.13)	40.96 (± 3.91)	0	0
5	0	0	4.9 (± 0.81)	83.2 (± 7)	0.78	16	3.1	18.9	2.0	51.3	0.1	0	0.902(± 0.12)	41.78 (± 3.52)	0	0
6	0	0	5.7 (± 0.54)	79.6 (± 9)	0.85	14	3.1	16.0	2.2	42.1	0.1	0	1.20(± 0.03)	49.18 (± 7.01)	0	0

All potentials referenced to Fc. All experiments performed with 0.1 M $TBAPF_6$ [a] – data based on triplicate data. Standard deviation given in parentheses [b] – data from single runs using conditions listed. [c]– data based on duplicate data. Standard deviation given in parentheses. [d] – This controls experiment was performed to test if the decomposition onto the electrode during CPE with **1** is capable of CO_2RR or HER. Recent research has shown Pt counter electrodes are capable of releasing Pt^{z+} ions into solution which can then deposit onto working electrodes and performed under catalytic conditions.[15–17] The electrode was first used in a 6h CPE with **1** then, without cleaning, transferred to fresh 1M TFE in DMF electrolyte without **1** present. The electrode was then tested for a second 6h CPE which showed no CO and very little H2 produced. The H2 produced would correspond to ~ 0.03 TON if using the concentration of **1** from the initial CPE, showing little contribution of the decomposition products toward the observed CO_2RR and HER.

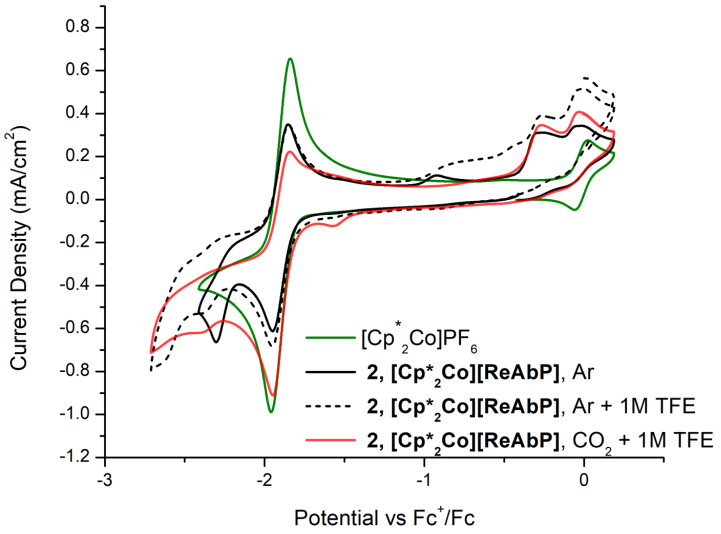

Fig S37: the cyclic voltammogram of complex **2** in DMF collected with WE: GC disk, CE: Pt mesh, RE: Ag/AgCl pseudoreference. Green trace is $[Cp^*_2Co]PF_6$ as purchased from Sigma-Aldrich

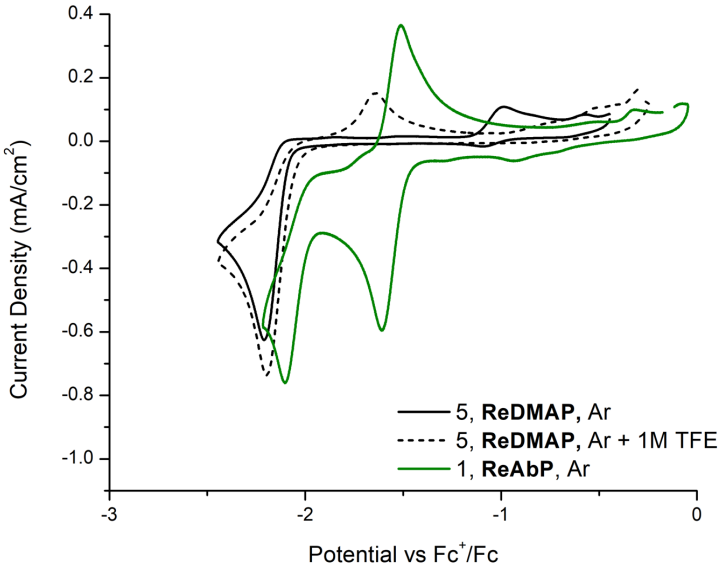

Fig S38: The CV of **5** in DMF, 0.1M $TBAPF_6$, Ar with overlay 1 under identical conditions. WE: GC disk, CE: Pt mesh, RE: Ag/AgCl pseudoreference

UV-Vis Spectra

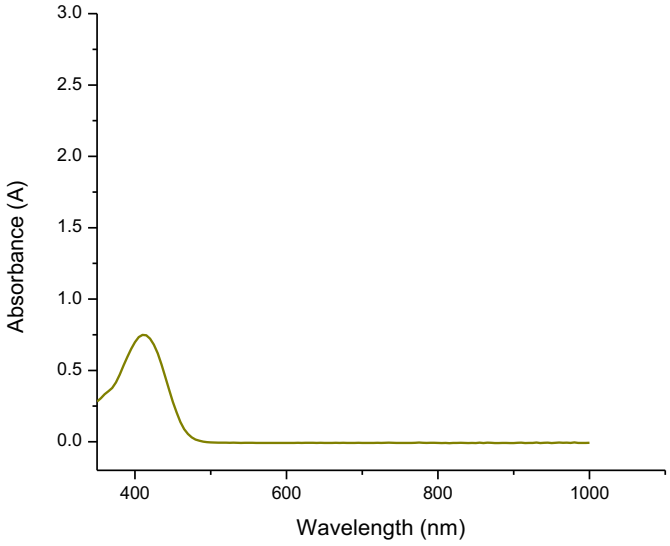

Fig S39: The UV-Vis spectrum of **ii** in THF

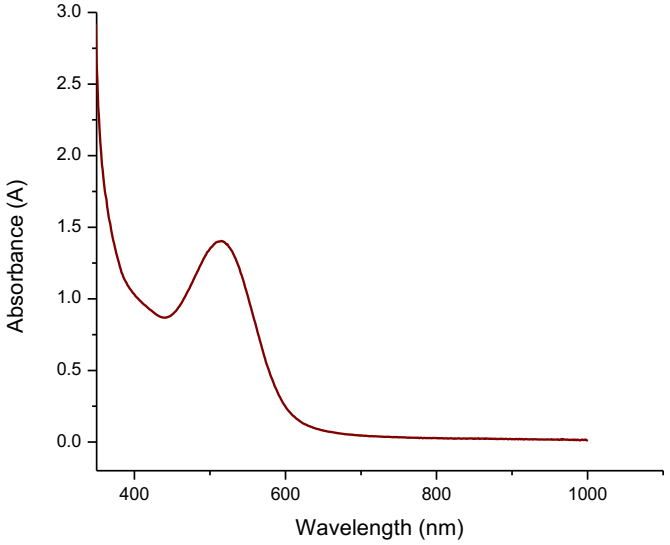

Fig S40: The UV-Vis spectrum of **1** in DMF

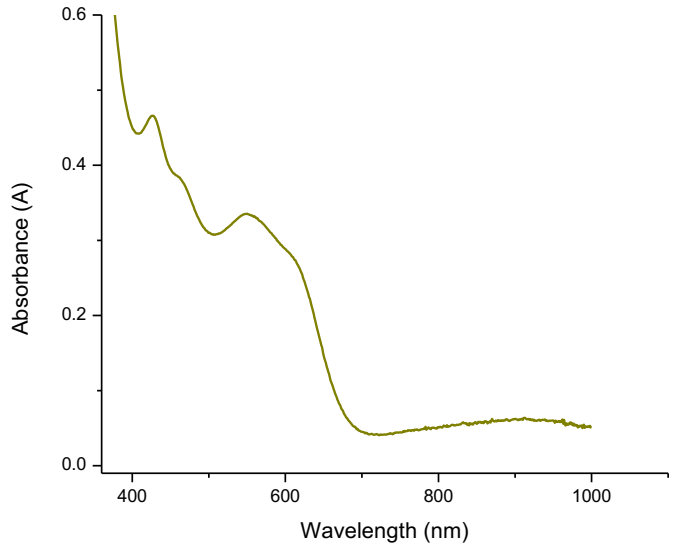

Fig S41: The UV-Vis spectrum of 2 in THF

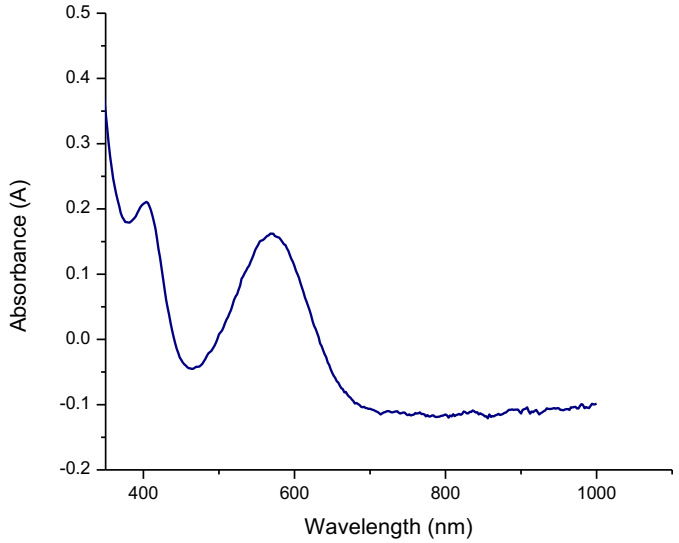

Fig S42: The UV-Vis spectrum of **4** in DMF

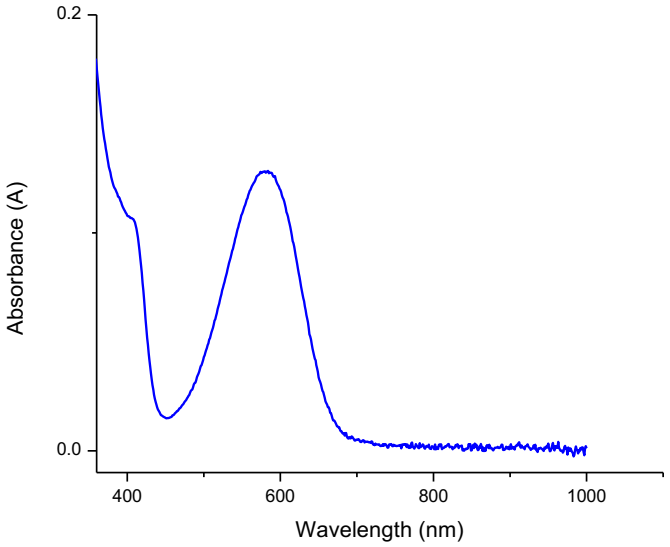

Fig S43: The UV-Vis spectrum of **5** in THF

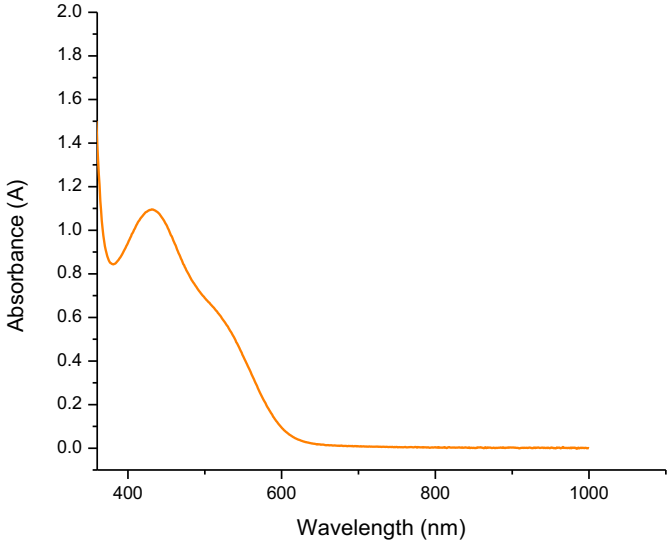

Fig S44: The UV-Vis spectrum of **6** in THF

Supplementary Crystal Structures and X-ray Crystallography Tables

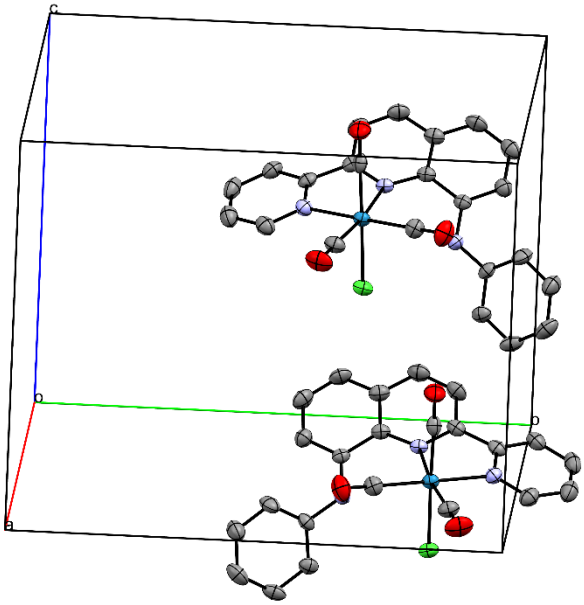

Figure S45: Both helically chiral isomers are seen in the unit cell of **1**.

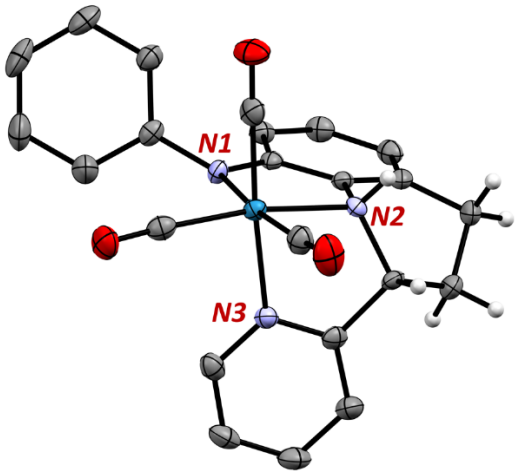

Figure S46. Single crystal X-ray structure of the dearomatized Re(I) complex **3** is shown with ellipsoids at 50% with solvent and most hydrogen atoms removed for clarity. Hydrogens shown are to highlight the dearomatization of the quinoline backbone. Selected bond lengths (Å): Re1-N1 = 2.154(2), Re1-N2 = 2.198(3), Re1-N3 = 2.195 (3).

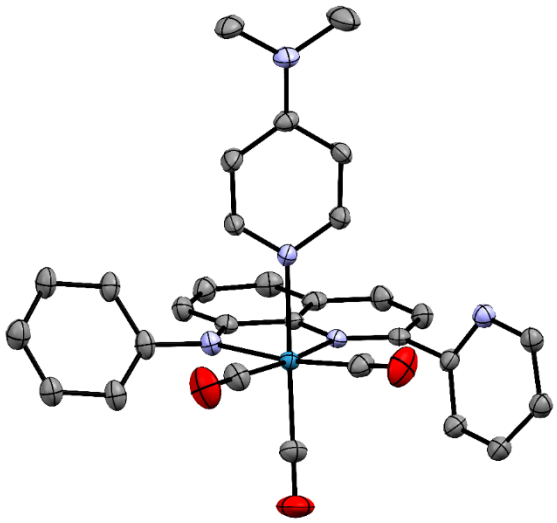

Fig S47: The X-ray crystal structure of **5**, hydrogens and solvent removed for clarity.

Table 2 Crystal data and structure refinement for compounds **1,2,4**			
Identification code	**1**	**2**	**4**
Empirical formula	$C_{23}H_{15}ClN_3O_3Re$	$C_{55}H_{54}ClCoF_2N_3O_3Re$	$C_{25.5}H_{20}N_3O_3Re$
Formula weight	603.03	1123.59	602.64
Temperature/K	296.15	173.0	173.0
Crystal system	monoclinic	orthorhombic	monoclinic
Space group	$P2_1/n$	Cmcm	I2/a
a/Å	11.7750(9)	21.5535(17)	19.8011(5)
b/Å	15.4255(12)	21.0599(7)	10.7352(3)
c/Å	12.1047(9)	21.3570(14)	21.1945(6)
α/°	90	90	90
β/°	104.6390(10)	90	100.5883(13)
γ/°	90	90	90
Volume/Å^3	2127.3(3)	9694.3(10)	4428.6(2)
Z	4	8	8
ρ_{calc}g/cm^3	1.883	1.540	1.808
μ/mm^{-1}	5.868	8.438	11.008
F(000)	1160.0	4528.0	2344.0
Crystal size/mm^3	0.188 × 0.162 × 0.122	0.252 × 0.234 × 0.052	0.168 × 0.075 × 0.03
Radiation	MoKα (λ = 0.71073)	CuKα (λ = 1.54178)	CuKα (λ = 1.54178)
2Θ range for data collection/°	4.312 to 55.752	5.868 to 133.104	8.488 to 133.152
Index ranges	$-15 \leq h \leq 15$, $-20 \leq k \leq 20$, $-15 \leq l \leq 15$	$-13 \leq h \leq 25$, $-25 \leq k \leq 24$, $-25 \leq l \leq 23$	$-23 \leq h \leq 23$, $-12 \leq k \leq 12$, $-25 \leq l \leq 25$
Reflections collected	25903	17382	3809

Independent reflections	5077 [R_{int} = 0.0497, R_{sigma} = 0.0385]	4426 [R_{int} = 0.0909, R_{sigma} = 0.0827]	3809 [R_{int} = 0.0644, R_{sigma} = 0.0720]
Data/restraints/parameters	5077/0/280	4426/937/486	3809/164/349
Goodness-of-fit on F^2	0.717	1.026	1.064
Final R indexes [I>=2σ (I)]	R_1 = 0.0264, wR_2 = 0.0814	R_1 = 0.0619, wR_2 = 0.1433	R_1 = 0.0360, wR_2 = 0.0843
Final R indexes [all data]	R_1 = 0.0405, wR_2 = 0.0968	R_1 = 0.0971, wR_2 = 0.1615	R_1 = 0.0395, wR_2 = 0.0866
Largest diff. peak/hole / e $Å^{-3}$	1.22/-0.58	1.67/-1.34	1.50/-0.97

Table 2 Crystal data and structure refinement for compounds **7,** dearomatized Re complex, 3, and **9**			
Identification code	**5**	3	**6**
Empirical formula	$C_{36}H_{30}N_5O_3Re$	$C_{29}H_{18}D_6N_3O_3Re$	C51H46Cl2N6O9Re2
Formula weight	766.85	654.75	1330.24
Temperature/K	173.0	173.0	173
Crystal system	monoclinic	triclinic	triclinic
Space group	$P2_1/c$	P-1	P-1
a/Å	8.8205(8)	9.6071(9)	10.6487(7)
b/Å	13.4145(12)	11.7517(10)	14.8830(10)
c/Å	26.571(2)	12.1793(11)	17.1392(12)
α/°	90	81.0430(10)	73.3670(10)
β/°	91.8983(11)	80.2040(10)	79.1560(10)
γ/°	90	67.7730(10)	76.0790(10)
Volume/$Å^3$	3142.3(5)	1248.00(19)	2505.3(3)
Z	4	2	2
ρ_{calc}g/cm^3	1.621	1.742	1.763
μ/mm^{-1}	3.912	4.905	4.996
F(000)	1520.0	636.0	1300.0
Crystal size/mm^3	0.284 × 0.228 × 0.048	0.192 × 0.088 × 0.054	0.207 × 0.119 × 0.073
Radiation	MoKα (λ = 0.71073)	MoKα (λ = 0.71073)	MoKα (λ = 0.71073)
2Θ range for data collection/°	3.068 to 58.274	3.41 to 56.554	2.5 to 55.596
Index ranges	-12 ≤ h ≤ 12, -18 ≤ k ≤ 18, -36 ≤ l ≤ 36	-12 ≤ h ≤ 12, -15 ≤ k ≤ 15, -16 ≤ l ≤ 16	-13 ≤ h ≤ 13, -19 ≤ k ≤ 19, -22 ≤ l ≤ 22
Reflections collected	42912	18767	48489
Independent reflections	8443 [R_{int} = 0.0499, R_{sigma} = 0.0395]	6183 [R_{int} = 0.0395, R_{sigma} = 0.0437]	11853 [Rint = 0.0690, Rsigma = 0.0629]
Data/restraints/parameters	8443/962/531	6183/72/361	11853/0/639
Goodness-of-fit on F^2	1.041	1.019	0.998
Final R indexes [I>=2σ (I)]	R_1 = 0.0262, wR_2 = 0.0488	R_1 = 0.0259, wR_2 = 0.0492	R1 = 0.0330, wR2 = 0.0556

Final R indexes [all data]	R_1 = 0.0388, wR_2 = 0.0519	R_1 = 0.0338, wR_2 = 0.0516	R1 = 0.0565, wR2 = 0.0624
Largest diff. peak/hole / e $Å^{-3}$	0.74/-0.52	0.85/-1.04	1.02/-0.80

References

(1) Lalancette, J.-M.; Rollin, G.; Dumas, P. Metals Intercalated in Graphite. I. Reduction and Oxidation. *Can. J. Chem.* **1972**, *50* (18), 3058–3062. https://doi.org/10.1139/v72-485.

(2) Tong, L.; Zong, R.; Thummel, R. P. Visible Light-Driven Hydrogen Evolution from Water Catalyzed by A Molecular Cobalt Complex. *J. Am. Chem. Soc.* **2014**, *136* (13), 4881–4884. https://doi.org/10.1021/ja501257d.

(3) LeBlanc, F. A.; Piers, W. E.; Parvez, M. Selective Hydrosilation of CO 2 to a Bis(Silylacetal) Using an Anilido Bipyridyl-Ligated Organoscandium Catalyst. *Angew. Chem.* **2014**, *126* (3), 808–811. https://doi.org/10.1002/ange.201309094.

(4) Smieja, J. M.; Kubiak, C. P. Re(Bipy-TBu)(CO) 3 Cl−improved Catalytic Activity for Reduction of Carbon Dioxide: IR-Spectroelectrochemical and Mechanistic Studies. *Inorg. Chem.* **2010**, *49* (20), 9283–9289. https://doi.org/10.1021/ic1008363.

(5) Bordwell, F. G.; Algrim, D. Nitrogen Acids. 1. Carboxamides and Sulfonamides. *J. Org. Chem.* **1976**, *41* (14), 2507–2508. https://doi.org/10.1021/jo00876a042.

(6) Kolthoff, I. M.; Chantooni, M. K.; Bhowmik, S. Dissociation Constants of Uncharged and Monovalent Cation Acids in Dimethyl Sulfoxide. *J. Am. Chem. Soc.* **1968**, *90* (1), 23–28. https://doi.org/10.1021/ja01003a005.

(7) Crampton, M. R.; Robotham, I. A. Acidities of Some Substituted Ammonium Ions in Dimethyl Sulfoxide†. *J. Chem. Res.* **1997**, No. 1, 22–23. https://doi.org/10.1039/a606020j.

(8) Benoit, R. L.; Lefebvre, D.; Fréchette, M. Basicity of 1,8-Bis(Dimethylamino)Naphthalene and 1,4-Diazabicyclo[2.2.2]Octane in Water and Dimethylsulfoxide. *Can. J. Chem.* **1987**, *65* (5), 996–1001. https://doi.org/10.1139/v87-170.

(9) Bordwell, F. G. Equilibrium Acidities in Dimethyl Sulfoxide Solution. *Acc. Chem. Res.* **1988**, *21* (12), 456–463. https://doi.org/10.1021/ar00156a004.

(10) Maran, F.; Celadon, D.; Severin, M. G.; Vianello, E. Electrochemical Determination of the PKa of Weak Acids in N,N-Dimethylformamide. *J. Am. Chem. Soc.* **1991**, *113* (24), 9320–9329. https://doi.org/10.1021/ja00024a041.

(11) Rõõm, E.-I.; Kaljurand, I.; Leito, I.; Rodima, T.; Koppel, I. A.; Vlasov, V. M. Acid−Base Equilibria in Nonpolar Media. 3. Expanding the Spectrophotometric Acidity Scale in Heptane. *J. Org. Chem.* **2003**, *68* (20), 7795–7799. https://doi.org/10.1021/jo0343477.

(12) Leito, I.; Rodima, T.; Koppel, I. A.; Schwesinger, R.; Vlasov, V. M. Acid−Base Equilibria in Nonpolar Media. 1. A Spectrophotometric Method for Acidity Measurements in Heptane. *J. Org. Chem.* **1997**, *62* (24), 8479–8483. https://doi.org/10.1021/jo9713013.

(13) Clark, M. L.; Cheung, P. L.; Lessio, M.; Carter, E. A.; Kubiak, C. P. Kinetic and Mechanistic Effects of Bipyridine (Bpy) Substituent, Labile Ligand, and Brønsted Acid on Electrocatalytic CO_2 Reduction by Re(Bpy) Complexes. *ACS Catal.* **2018**, *8* (3), 2021–2029. https://doi.org/10.1021/acscatal.7b03971.

(14) Warren, J. J.; Tronic, T. A.; Mayer, J. M. Thermochemistry of Proton-Coupled Electron Transfer Reagents and Its Implications. *Chem. Rev.* **2010**, *110* (12), 6961–7001. https://doi.org/10.1021/cr100085k.

(15) Dong, G.; Fang, M.; Wang, H.; Yip, S.; Cheung, H.-Y.; Wang, F.; Wong, C.-Y.; Tak Chu, S.; C. Ho, J. Insight into the Electrochemical Activation of Carbon-Based Cathodes for Hydrogen Evolution Reaction. *J. Mater. Chem. A* **2015**, *3* (24), 13080–13086. https://doi.org/10.1039/C5TA02551F.

(16) Chen, R.; Yang, C.; Cai, W.; Wang, H.-Y.; Miao, J.; Zhang, L.; Chen, S.; Liu, B. Use of Platinum as the Counter Electrode to Study the Activity of Nonprecious Metal Catalysts for the Hydrogen Evolution Reaction. *ACS Energy Lett.* **2017**, *2* (5), 1070–1075. https://doi.org/10.1021/acsenergylett.7b00219.

(17) Jerkiewicz, G. Applicability of Platinum as a Counter-Electrode Material in Electrocatalysis Research. *ACS Catal.* **2022**, *12* (4), 2661–2670. https://doi.org/10.1021/acscatal.1c06040.